"Nitrogen demand, supply, and acquisition strategy control plant responses to elevated CO_2 at different scales"

Evan A. Perkowski[1,*], Ezinwanne Ezekannagha[1], Nicholas G. Smith[1]

[1]Department of Biological Sciences, Texas Tech University, Lubbock, TX

[*]Corresponding author:
2901 Main St.
Lubbock, TX, 79409
Email: evan.a.perkowski@ttu.edu

ORCIDs: Evan A. Perkowski (0000-0002-9523-8892), Ezinwanne Ezekannagha (0000-0001-7469-949X), Nicholas G. Smith (0000-0001-7048-4387)

Abstract

Plants respond to elevated atmospheric CO_2 concentrations by reducing leaf nitrogen content and photosynthetic capacity – patterns that correspond with increased net photosynthesis rates, total leaf area, and total biomass. Nitrogen supply has been hypothesized to be the primary factor controlling these responses, as nitrogen availability limits net primary productivity globally. Recent work using evo-evolutionary optimality theory suggests that leaf photosynthetic responses to elevated CO_2 are independent of nitrogen supply and are instead driven by leaf nitrogen demand to build and maintain photosynthetic enzymes, which optimizes resource allocation to photosynthetic capacity and maximizes allocation to growth. Here, *Glycine max* L. (Merr) seedlings were grown under two CO_2 concentrations, with and without inoculation with *Bradyrhizobium japonicum*, and across nine soil nitrogen fertilization treatments in a full-factorial growth chamber experiment to reconcile the role of nitrogen supply and demand on leaf and whole-plant responses to elevated CO_2. After seven weeks, elevated CO_2 increased net photosynthesis rates despite reduced leaf nitrogen content and maximum rates of Ribulose-1,5-bisphosphate (RuBP) carboxylase/oxygenase (Rubisco) carboxylation and electron transport for RuBP regeneration. Effects of elevated CO_2 on net photosynthesis and indices of photosynthetic capacity were independent of nitrogen fertilization and inoculation. However, increasing

nitrogen fertilization enhanced positive effects of elevated CO_2 on total leaf area and total biomass due to increased nitrogen uptake and reduced carbon costs to acquire nitrogen. Whole-plant responses to elevated CO_2 were not modified by inoculation across the nitrogen fertilization gradient, as plant investment toward symbiotic nitrogen fixation was similar between CO_2 treatments. These results indicate that leaf nitrogen demand to build and maintain photosynthetic enzymes drives leaf photosynthetic responses to elevated CO_2, while nitrogen supply regulates whole-plant responses. Our findings build on previous work suggesting that terrestrial biosphere models may improve simulations of photosynthetic processes under future novel environments by adopting optimality principles.

Keywords

acclimation, eco-evolutionary optimality, growth chamber, least-cost theory, nitrogen acquisition strategy, photosynthesis, plant functional ecology, whole-plant growth

Introduction

Terrestrial ecosystems are regulated by complex carbon and nitrogen cycles. As a result, terrestrial biosphere models, which are beginning to include coupled carbon and nitrogen cycles (Shi *et al.*, 2016; Davies-Barnard *et al.*, 2020; Braghiere *et al.*, 2022), must accurately represent these cycles under different environmental scenarios to reliably simulate carbon and nitrogen fluxes (Oreskes *et al.*, 1994; Prentice *et al.*, 2015). While the inclusion of coupled carbon and nitrogen cycles in terrestrial biosphere models was intended to improve model reliability, large uncertainty in the role of nitrogen availability and nitrogen acquisition strategy on leaf and whole plant responses to increasing atmospheric CO_2 concentrations persists (Arora *et al.*, 2020; Davies-Barnard *et al.*, 2020; Kou-Giesbrecht *et al.*, 2023), contributing to widespread divergence in future carbon and nitrogen flux simulations across terrestrial biosphere models (Hungate *et al.*, 2003; Friedlingstein *et al.*, 2014; Zaehle *et al.*, 2014; Wieder *et al.*, 2015; Meyerholt *et al.*, 2020).

Over the past few decades, numerous studies have sought to elucidate plant responses to elevated CO_2, revealing consistent leaf and whole-plant patterns. At the leaf level, C_3 plants grown under elevated CO_2 exhibit increased net photosynthesis rates compared to plants grown under ambient CO_2 (Medlyn *et al.*, 1999; Ainsworth & Long, 2005; Bernacchi *et al.*, 2005; Lee

63 *et al.*, 2011; Poorter *et al.*, 2022). These patterns correspond with reduced mass- and area-based
64 leaf nitrogen content, increased leaf mass per area, reduced stomatal conductance, and reduced
65 photosynthetic capacity, yielding increased photosynthetic nitrogen-use efficiency and water-use
66 efficiency (Curtis, 1996; Drake *et al.*, 1997; Medlyn *et al.*, 1999; Ainsworth & Long, 2005;
67 Ainsworth & Rogers, 2007; Lee *et al.*, 2011; Pastore *et al.*, 2019; Poorter *et al.*, 2022). At the
68 whole-plant level, C_3 plants grown under elevated CO_2 exhibit increased total leaf area, which
69 supports greater net primary productivity and total biomass compared to plants grown under
70 ambient CO_2 (Coleman *et al.*, 1993; Ainsworth *et al.*, 2002; Ainsworth & Rogers, 2007; Finzi *et*
71 *al.*, 2007; Poorter *et al.*, 2022). Some experiments suggest that elevated CO_2 increases
72 belowground carbon allocation and the ratio of root biomass to shoot biomass compared to plants
73 grown under ambient CO_2 (Nie *et al.*, 2013), though this allocation response is not consistently
74 observed (Luo *et al.*, 1994; Poorter *et al.*, 2022).
75 Despite consistent plant responses to elevated CO_2 documented across experiments,
76 mechanisms that drive these responses remain unresolved. Some have hypothesized that plant
77 responses to elevated CO_2 are constrained by nitrogen availability, as net primary productivity is
78 limited by nitrogen availability globally (Vitousek & Howarth, 1991; LeBauer & Treseder,
79 2008). The progressive nitrogen limitation hypothesis predicts that elevated CO_2 will increase
80 plant nitrogen uptake to support greater net primary productivity, which will cause nitrogen
81 availability to decline over time (Luo *et al.*, 2004). The hypothesis predicts that this response
82 should increase growth and net primary productivity under elevated CO_2 over short time scales
83 that dampen with time as nitrogen becomes progressively more limiting and stored in longer-
84 lived tissues. Growth responses to elevated CO_2 expected from the progressive nitrogen
85 limitation hypothesis have received some support from free-air CO_2 enrichment experiments
86 (Reich *et al.*, 2006; Norby *et al.*, 2010), though these patterns are not consistently observed
87 (Finzi *et al.*, 2006, 2007; Moore *et al.*, 2006; Liang *et al.*, 2016).
88 Assuming positive relationships between soil nitrogen availability, leaf nitrogen content,
89 and photosynthetic capacity (Field & Mooney, 1986; Evans, 1989; Evans & Seemann, 1989;
90 Walker *et al.*, 2014; Firn *et al.*, 2019; Liang *et al.*, 2020), the progressive nitrogen limitation
91 hypothesis implies that reductions in nitrogen availability over time might explain why C_3 plants
92 exhibit decreased leaf nitrogen content and photosynthetic capacity under elevated CO_2.
93 However, results from free-air CO_2 enrichment experiments show that reductions in leaf nitrogen

content and photosynthetic capacity under elevated CO_2 are decoupled from changes in nitrogen availability (Crous *et al.*, 2010; Lee *et al.*, 2011; Pastore *et al.*, 2019). Additionally, variance in leaf nitrogen and photosynthetic capacity across environmental gradients tends to be more strongly determined through aboveground growth conditions that set demand to build and maintain photosynthetic enzymes than through changes in soil resource availability (Dong *et al.*, 2017, 2020, 2022a; Smith *et al.*, 2019; Smith & Keenan, 2020; Paillassa *et al.*, 2020; Peng *et al.*, 2021; Querejeta *et al.*, 2022; Westerband *et al.*, 2023; Waring *et al.*, 2023). These patterns indicate that leaf photosynthetic responses to elevated CO_2 may be a product of altered leaf nitrogen demand to build and maintain photosynthetic enzymes and may not be as strongly linked to changes in nitrogen availability.

Eco-evolutionary optimality theory provides a framework for understanding how leaf photosynthetic responses to elevated CO_2 may be determined through demand to build and maintain photosynthetic enzymes (Harrison *et al.*, 2021). Merging photosynthetic least-cost (Wright *et al.*, 2003; Prentice *et al.*, 2014) and optimal coordination (Chen *et al.*, 1993; Maire *et al.*, 2012) theories, eco-evolutionary optimality theory posits that reduced leaf nitrogen allocation under elevated CO_2 is the downstream result of a stronger downregulation in the maximum rate of Ribulose-1,5-bisphosphate (RuBP) carboxylase/oxygenase (Rubisco) carboxylation (V_{cmax}) than the maximum rate of electron transport for RuBP regeneration (J_{max}), which reduces leaf nitrogen demand to build and maintain photosynthetic enzymes. Optimal leaf nitrogen allocation to photosynthetic capacity allows plants to make more efficient use of available light while avoiding overinvestment in Rubisco, which has high nitrogen and energetic costs of construction and maintenance (Evans, 1989; Sage, 1994; Evans & Clarke, 2019). Such optimal leaf nitrogen allocation responses to elevated CO_2 increases photosynthetic nitrogen-use efficiency and allows increased net photosynthesis rates to be achieved through increasingly equal co-limitation of Rubisco carboxylation and electron transport for RuBP regeneration (Chen *et al.*, 1993; Maire *et al.*, 2012; Wang *et al.*, 2017; Smith *et al.*, 2019). The expected optimal leaf response to elevated CO_2 has received some empirical support (Crous *et al.*, 2010; Lee *et al.*, 2011; Smith & Keenan, 2020; Harrison *et al.*, 2021; Dong *et al.*, 2022b; Cui *et al.*, 2023), though no studies have connected these patterns with concurrently measured whole-plant responses.

The eco-evolutionary optimality hypothesis deviates from the progressive nitrogen limitation hypothesis by indicating that photosynthetic responses to elevated CO_2 are driven by

leaf nitrogen demand to build and maintain photosynthetic enzymes and are independent of changes in soil nitrogen supply. However, the eco-evolutionary optimality hypothesis does not discount the role of soil nitrogen availability on whole-plant responses to elevated CO_2, where the expected optimal strategy in response to elevated CO_2 is to allocate surplus nitrogen not needed to satisfy leaf nitrogen demand toward the construction of a greater quantity of optimally coordinated leaves and other plant organs. Thus, whether the supply-driven progressive nitrogen limitation hypothesis or demand-driven eco-evolutionary optimality hypothesis controls plant responses to elevated CO_2 may be a matter of scale, where leaf photosynthetic responses to elevated CO_2 are determined through demand to build and maintain photosynthetic enzymes and whole-plant responses to elevated CO_2 are regulated by changes in nitrogen supply.

Plants allocate carbon belowground in exchange for nutrients through different nutrient acquisition strategies, including direct uptake pathways or symbioses with mycorrhizal fungi and symbiotic nitrogen-fixing bacteria (Gutschick, 1981; Smith & Read, 2008). Carbon costs to acquire nitrogen, or the amount of carbon allocated belowground per unit nitrogen acquired, vary in species with different nitrogen acquisition strategies and are dependent on environmental factors such as atmospheric CO_2, temperature, light availability, and nutrient availability (Brzostek *et al.*, 2014; Terrer *et al.*, 2018; Allen *et al.*, 2020; Eastman *et al.*, 2021; Perkowski *et al.*, 2021; Lu *et al.*, 2022; Peng *et al.*, 2023). Therefore, nitrogen acquisition strategy cannot be ignored when considering effects of nitrogen availability on plant responses to elevated CO_2. To date, few studies account for acquisition strategy when considering the role of nitrogen availability on leaf and whole-plant responses to elevated CO_2 (e.g., Terrer *et al.*, 2016, 2018; Smith & Keenan, 2020). Such studies found that nitrogen acquisition strategies with reduced carbon costs to acquire nitrogen may buffer the effect of nitrogen limitation at the whole-plant level (Terrer *et al.*, 2018), but leaf-level responses remain inconsistent (Terrer *et al.*, 2018; Smith & Keenan, 2020).

Here, we conducted a growth chamber experiment using *Glycine max* L. (Merr.) seedlings grown under full factorial combinations of two CO_2 concentrations, two inoculation treatments, and nine soil nitrogen fertilization treatments to reconcile the role of nitrogen supply and demand on plant responses to elevated CO_2. We used this experimental setup to test the following hypotheses:

155 (1) Following the demand-driven eco-evolutionary optimality hypothesis, elevated CO_2 will
156 downregulate V_{cmax} more strongly than J_{max}, increasing J_{max}:V_{cmax} and allowing increased
157 net photosynthesis rates to approach equal co-limitation of Rubisco carboxylation and
158 electron transport for RuBP regeneration. Leaf photosynthetic responses to elevated CO_2
159 will be independent of nitrogen fertilization and inoculation treatment and will
160 correspond with increased photosynthetic nitrogen-use efficiency.
161 (2) Following the supply-driven nitrogen limitation hypothesis, positive effects of elevated
162 CO_2 on total leaf area and total biomass will be enhanced with increasing nitrogen
163 fertilization due to increased plant nitrogen uptake and reduced carbon costs to acquire
164 nitrogen. Inoculation with symbiotic nitrogen-fixing bacteria will enhance positive
165 growth responses to elevated CO_2, though these responses will only be apparent under
166 low nitrogen fertilization levels where individuals will have increased investment in
167 nitrogen acquisition through symbiotic nitrogen fixation.
168
169 **Methods**
170 *Seed treatments and experimental design*
171 *Glycine max* seeds were planted in 144 6-liter surface sterilized pots (NS-600, Nursery Supplies,
172 Orange, CA, USA) containing a steam-sterilized 70:30 volume: volume mix of *Sphagnum* peat
173 moss (Premier Horticulture, Quakertown, PA, USA) to sand (Pavestone, Atlanta, GA, USA).
174 Before planting, all *G. max* seeds were surface sterilized in 2% sodium hypochlorite for 3
175 minutes, followed by three separate 3-minute washes with ultrapure water (MilliQ 7000;
176 MilliporeSigma, Burlington, MA USA). Subsets of surface-sterilized seeds were inoculated with
177 *Bradyrhizobium japonicum* (Verdesian N-Dure™ Soybean, Cary, NC, USA) in a slurry
178 following manufacturer recommendations (3.12 g inoculant and 241 g ultrapure water per 1 kg
179 seed).
180 Seventy-two pots were randomly planted with surface-sterilized seeds inoculated with *B.*
181 *japonicum*, while the remaining 72 pots were planted with surface-sterilized uninoculated seeds.
182 Thirty-six pots in each inoculation treatment were randomly placed in one of two atmospheric
183 CO_2 treatments (420 and 1000 μmol mol^{-1} CO_2). Plants in each unique inoculation-by-CO_2
184 treatment combination randomly received one of nine nitrogen fertilization treatments equivalent
185 to 0 (0 mM), 35 (2.5 mM), 70 (5 mM), 105 (7.5 mM), 140 (10 mM), 210 (15 mM), 280 (20

186 mM), 350 (25 mM), or 630 ppm (45 mM) N. Nitrogen fertilization treatments were created using
187 a modified Hoagland's solution (Hoagland & Arnon, 1950) designed to keep concentrations of
188 all other macronutrients and micronutrients equivalent across treatments (Table S1). Plants
189 received the same nitrogen fertilization treatment twice per week in 150 mL doses as topical
190 agents to the soil surface.
191
192 *Growth chamber conditions*
193 Plants were randomly placed in one of six Percival LED-41L2 growth chambers (Percival
194 Scientific Inc., Perry, IA, USA) over two experimental iterations due to chamber space
195 limitation. Two iterations were conducted such that one iteration included all plants grown under
196 elevated CO_2 plants, and the second iteration included all plants grown under ambient CO_2.
197 Average (± SD) CO_2 concentrations across chambers throughout the experiment were 439±5
198 μmol mol^{-1} CO_2 for the ambient treatment and 989±4 μmol mol^{-1} CO_2 for the elevated treatment.
199 Daytime growth conditions were simulated using a 16-hour photoperiod, with incoming
200 light radiation set to chamber maximum (mean±SD: 1230±12 μmol m^{-2} s^{-1} across chambers), air
201 temperature set to 25°C, and relative humidity set to 50%. The remaining 8-hour period
202 simulated nighttime growing conditions, with incoming light radiation set to 0 μmol m^{-2} s^{-1},
203 chamber temperature set to 17°C, and relative humidity set to 50%. Transitions between daytime
204 and nighttime growing conditions were simulated by ramping incoming light radiation in 45-
205 minute increments and temperature in 90-minute increments over a 3-hour period (Table S2).
206 Plants grew under average (± SD) daytime light intensity of 1049±27 μmol m^{-2} s^{-1},
207 including ramping periods. In the elevated CO_2 iteration, plants grew under 24.0±0.2°C during
208 the day, 16.4±0.8°C during the night, and 51.6±0.4% relative humidity. In the ambient CO_2
209 iteration, plants grew under 23.9±0.2°C during the day, 16.0±1.4°C during the night, and
210 50.3±0.2% relative humidity. Within each experiment iteration, any differences in climate
211 conditions across the six chambers were accounted for by shuffling the same group of plants
212 throughout the growth chambers. This process was done by iteratively moving the group of
213 plants on the top rack of a chamber to the bottom rack of the same chamber, while
214 simultaneously moving the group of plants on the bottom rack of a chamber to the top rack of the
215 adjacent chamber. Plants were moved within and across chambers daily during each experiment
216 iteration.

Leaf gas exchange measurements

Leaf gas exchange measurements were collected on the seventh week of development, before the onset of reproduction. All gas exchange measurements were collected on the center leaf of the most recent fully expanded trifoliate leaf set using LI-6800 portable photosynthesis machines configured with a 6800-01A fluorometer head and 6 cm^2 aperture (LI-COR Biosciences, Lincoln, NE, USA). Specifically, net photosynthesis (A_{net}; µmol m^{-2} s^{-1}), stomatal conductance (g_{sw}; mol m^{-2} s^{-1}), and intercellular CO_2 (C_i; µmol mol^{-1}) concentrations were measured across a range of atmospheric CO_2 concentrations (i.e., an A_{net}/C_i curve) using the Dynamic Assimilation™ Technique. The Dynamic Assimilation™ Technique corresponds well with traditional steady-state A_{net}/C_i curves in *G. max* (Saathoff & Welles, 2021). A_{net}/C_i curves were generated along a reference CO_2 ramp down from 420 µmol mol^{-1} CO_2 to 20 µmol mol^{-1} CO_2, followed by a ramp up from 420 µmol mol^{-1} CO_2 to 1620 µmol mol^{-1} CO_2 after a 90-second wait period at 420 µmol mol^{-1} CO_2. The ramp rate for each curve was set to 200 µmol mol^{-1} min^{-1}, logging every five seconds, which generated 96 data points per response curve. All A_{net}/C_i curves were generated after A_{net} and g_{sw} stabilized in a LI-6800 cuvette set to a 500 mol s^{-1} flow rate, 10000 rpm mixing fan speed, 1.5 kPa vapor pressure deficit, 25°C leaf temperature, 2000 µmol m^{-2} s^{-1} incoming light radiation, and initial reference CO_2 set to 420 µmol mol^{-1}.

Snapshot A_{net} measurements were extracted from each A_{net}/C_i curve, both at a common CO_2 concentration, 420 µmol mol^{-1} CO_2 ($A_{net,420}$; µmol m^{-2} s^{-1}), and under each individual's growth CO_2 concentration, 420 and 1000 µmol mol^{-1} CO_2 ($A_{net,growth}$; µmol m^{-2} s^{-1}). Dark respiration (R_d; µmol m^{-2} s^{-1}) measurements were collected with the same leaf used to generate A_{net}/C_i curves following at least 30 minutes of darkness. Measurements were collected on a 5-second log interval for 60 seconds after the leaf stabilized in a LI-6800 cuvette set to a 500 mol s^{-1} flow rate, 10000 rpm mixing fan speed, 1.5 kPa vapor pressure deficit, 25°C leaf temperature, and 420 µmol mol^{-1} reference CO_2 concentration (regardless of CO_2 treatment), with incoming light radiation set to 0 µmol m^{-2} s^{-1}. A single dark respiration value was determined for each leaf by calculating the mean dark respiration value across the logging interval.

A/C_i curve-fitting and parameter estimation

A_{net}/C_i curves were fit using the 'fitaci' function in the 'plantecophys' R package (Duursma, 2015). This function estimates the maximum rate of Rubisco carboxylation (V_{cmax}; µmol m^{-2} s^{-1}) and maximum rate of electron transport for RuBP regeneration (J_{max}; µmol m^{-2} s^{-1}) based on the Farquhar *et al.* (1980) biochemical model of C_3 photosynthesis. Triose phosphate utilization (TPU) limitation was included as an additional rate-limiting step in all curve fits after visually observing clear TPU limitation for most curves. All curve fits included measured dark respiration values. As A_{net}/C_i curves were generated using a common leaf temperature (25°C), curves were fit using Michaelis-Menten coefficients for Rubisco affinity to CO_2 (K_c; µmol mol^{-1}) and O_2 (K_o; mmol mol^{-1}), and the CO_2 compensation point (Γ^*; µmol mol^{-1}) reported in Bernacchi *et al.* (2001). Specifically, K_c was set to 404.9 µmol mol^{-1}, K_o was set to 278.4 µmol mol^{-1}, and Γ^* was set to 42.75 µmol mol^{-1}. For clarity, V_{cmax}, J_{max}, and R_d estimates are referenced throughout the rest of the paper as V_{cmax25}, J_{max25}, and R_{d25}.

Leaf trait measurements

The leaf used to generate A_{net}/C_i curves and dark respiration measurements was harvested immediately following gas exchange measurements. Images of each focal leaf were curated using a flat-bed scanner to determine fresh leaf area using the 'LeafArea' R package (Katabuchi, 2015), which automates leaf area calculations using ImageJ software (Schneider *et al.*, 2012). Post-processed images were visually assessed to check against errors in the automation process. Each leaf was dried at 65°C for at least 48 hours and subsequently weighed and ground until homogenized. Leaf mass per area (M_{area}; g m^{-2}) was calculated as the ratio of dry leaf biomass to fresh leaf area. Leaf nitrogen content (N_{mass}; gN g^{-1}) was quantified using a subsample of ground and homogenized leaf tissue through elemental combustion analysis (Costech-4010, Costech, Inc., Valencia, CA, USA). Leaf nitrogen content per unit leaf area (N_{area}; gN m^{-2}) was calculated by multiplying N_{mass} and M_{area}. Photosynthetic nitrogen-use efficiency ($PNUE_{growth}$; µmol CO_2 g^{-1} N s^{-1}) was estimated as the ratio of $A_{net,growth}$ to N_{area}.

Chlorophyll content was extracted from a second leaf in the same trifoliate leaf set as the leaf used to generate A_{net}/C_i curves. A cork borer was used to punch between 3-5 0.6 cm^2 disks from the leaf. Images of each set of leaf disks were curated using a flat-bed scanner to determine wet leaf area, again quantified using the 'LeafArea' R package (Katabuchi, 2015). Leaf disks were shuttled into a test tube containing 10 mL dimethyl sulfoxide, vortexed, and incubated at

278 65°C for 120 minutes (Barnes *et al.*, 1992). Incubated test tubes were vortexed again before
279 being loaded in 150 µL triplicate aliquots to a 96-well plate. Dimethyl sulfoxide was loaded in
280 each plate as a single 150 µL triplicate aliquot and used as a blank. Absorbance measurements at
281 649 nm (A_{649}) and 665 nm (A_{665}) were recorded in each well using a plate reader (Biotek Synergy
282 H1; Biotek Instruments, Winooski, VT USA), with triplicates averaged and corrected by the
283 mean of the blank absorbance value. Blank-corrected absorbance values were used to estimate
284 Chl_a (µg mL^{-1}) and Chl_b (µg mL^{-1}) following equations from Wellburn (1994):

285 $$Chl_a = 12.47A_{665} - 3.62A_{649} \quad (1)$$

286 and

287 $$Chl_b = 25.06A_{649} - 6.5A_{665} \quad (2)$$

288 Chl_a and Chl_b were converted to mmol mL^{-1} using the molar masses of chlorophyll *a* (893.51 g
289 mol^{-1}) and chlorophyll *b* (907.47 g mol^{-1}), then added together to calculate the total chlorophyll
290 content in dimethyl sulfoxide extractant (mmol mL^{-1}). Total chlorophyll content (mmol) was
291 determined by multiplying the total chlorophyll content in dimethyl sulfoxide by the volume of
292 dimethyl sulfoxide extractant (10 mL). Area-based chlorophyll content (Chl_{area}; mmol m^{-2}) was
293 then calculated by dividing the total chlorophyll content by the total area of the leaf disks.

294 Subsamples of ground and homogenized leaf tissue were sent to the University of
295 California-Davis Stable Isotope Facility to determine leaf $\delta^{13}C$ and $\delta^{15}N$ using an elemental
296 analyzer (Elementar vario MICRO cube elemental analyzer; Elementar Analysensysteme GmbH,
297 Langenselbold, Germany) interfaced to an isotope ratio mass spectrometer (PDZ Europa 20-20
298 Isotope Ratio Mass Spectrometer, Sercon Ltd., Chestshire, UK). Leaf $\delta^{13}C$ was used to estimate
299 the time-integrated ratio of leaf intercellular CO_2 concentration to atmospheric CO_2
300 concentration (χ, unitless) using leaf $\delta^{13}C$ and chamber air $\delta^{13}C$ following Farquhar *et al.* (1989):

301 $$\chi = \frac{\Delta^{13}C - a}{b - a} \quad (3)$$

302 where $\Delta^{13}C$ represents the relative difference between leaf $\delta^{13}C$ (‰) and air $\delta^{13}C$ (‰), and is
303 calculated as:

304 $$\Delta^{13}C = \frac{\delta^{13}C_{air} - \delta^{13}C_{leaf}}{1 + \delta^{13}C_{leaf}} \quad (4)$$

305 $\delta^{13}C_{air}$ is the chamber $\delta^{13}C$ air fractionation, *a* represents the fractionation between ^{12}C and ^{13}C
306 due to diffusion in air, assumed to be 4.4‰, and *b* represents the fractionation caused by Rubisco
307 carboxylation, assumed to be 27‰ (Farquhar *et al.*, 1989). $\delta^{13}C_{air}$ was quantified in each

chamber by collecting air samples in triplicate for each CO_2 treatment using a 20 mL syringe (Air-Tite Products Co., Inc., Virginia Beach, VA, USA). Each air sample was plunged into a manually evacuated 10 mL Exetainer (Labco Ltd., Lampeter, UK) and sent to the University of California-Davis Stable Isotope Facility, where $\delta^{13}C_{air}$ was determined using a gas inlet system (GasBenchII; Thermo Fisher Scientific, Waltham, MA, USA) coupled to an isotope ratio mass spectrometer (Thermo Finnigan Delta Plus XL; Thermo Fisher Scientific, Waltham, MA, USA). $\delta^{13}C_{air}$ for each CO_2 treatment was estimated by calculating the mean of the triplicate $\delta^{13}C_{air}$ samples within each chamber, then calculating the mean $\delta^{13}C_{air}$ across all chambers. Specifically, $\delta^{13}C_{air}$ was -8.81‰ for the ambient CO_2 treatment and -5.95‰ for the elevated CO_2 treatment.

Finally, the percent of leaf nitrogen acquired from the atmosphere (%N_{dfa}; %) was estimated using leaf $\delta^{15}N$ and the following equation adapted from Andrews *et al.* (2011):

$$\%N_{dfa} = \frac{\delta^{15}N_{direct} - \delta^{15}N_{sample}}{\delta^{15}N_{direct} - \delta^{15}N_{fixation}} \quad (5)$$

where $\delta^{15}N_{direct}$ refers to the $\delta^{15}N$ value from plants that exclusively acquired nitrogen via direct uptake, $\delta^{15}N_{sample}$ refers to an individual's leaf $\delta^{15}N$, and $\delta^{15}N_{fixation}$ refers to the $\delta^{15}N$ value from individuals that were entirely reliant on nitrogen fixation. $\delta^{15}N_{direct}$ was calculated as the mean leaf $\delta^{15}N$ of uninoculated individuals within each unique nitrogen fertilization-by-CO_2 treatment combination. Any individual with visual evidence of root nodule formation or nodule initiation was omitted from the calculation of $\delta^{15}N_{direct}$. $\delta^{15}N_{fixation}$ was calculated within each CO_2 treatment using the mean leaf $\delta^{15}N$ of inoculated individuals that received 0 ppm N. $\delta^{15}N_{fixation}$ was not calculated within each unique nitrogen fertilization-by-CO_2 treatment combination, as previous studies suggest decreased reliance on nitrogen fixation with increasing nitrogen fertilization (e.g., Perkowski *et al.*, 2021).

Whole-plant measurements

Seven weeks after experiment initiation and immediately following gas exchange measurements, all individuals were harvested, and biomass of major organ types (leaves, stems, roots, and nodules when present) were separated. Fresh leaf area of all harvested leaves was measured using a LI-3100C (LI-COR Biosciences, Lincoln, Nebraska, USA). Total fresh leaf area (cm^2) was calculated as the sum of all leaf areas, including the leaf used to collect gas exchange data and the leaf used to extract chlorophyll content. All harvested material was dried in an oven set

338 to 65°C for at least 48 hours to a constant mass, weighed, and ground to homogeneity. Leaves
339 and root nodules were ground using a mortar and pestle, while stems and roots were ground
340 using an E3300 Single Speed Mini Cutting Mill (Eberbach Corp., MI, USA). Total biomass (g)
341 was calculated as the sum of dry leaf, stem, root, and root nodule biomass. Carbon and nitrogen
342 content was measured for each organ type through elemental combustion (Costech-4010,
343 Costech, Inc., Valencia, CA, USA) using subsamples of ground and homogenized organ tissue.
344 The ratio of root nodule biomass to root biomass was calculated as an additional indicator of
345 investment toward symbiotic nitrogen fixation.
346 Following Perkowski *et al.* (2021), carbon costs to acquire nitrogen were quantified as
347 the ratio of belowground carbon biomass to total nitrogen biomass (N_{cost}; gC gN^{-1}). Belowground
348 carbon biomass (C_{bg}; gC) was calculated as the sum of root carbon biomass and root nodule
349 carbon biomass. Root carbon biomass and root nodule carbon biomass were calculated as the
350 product of the organ biomass and respective organ carbon content. Total nitrogen biomass (N_{wp};
351 gN) was calculated as the sum of total leaf, stem, root, and root nodule nitrogen biomass. Leaf,
352 stem, root, and root nodule nitrogen biomass was calculated as the product of the organ biomass
353 and respective organ nitrogen content. This calculation does not account for additional carbon
354 costs associated with respiration, root exudation, or root turnover, and therefore may
355 underestimate carbon costs to acquire nitrogen (Perkowski *et al.*, 2021).
356
357 *Statistical analyses*
358 Uninoculated plants that had substantial root nodule formation (root nodule biomass: root
359 biomass values greater than 0.05 g g^{-1}) were removed from analyses under the assumption that
360 plants were either incompletely sterilized or were colonized by symbiotic nitrogen-fixing
361 bacteria from neighboring plants in the chamber. This decision resulted in the removal of sixteen
362 plants from the analysis: two plants in the elevated CO_2 treatment that received 35 ppm N, three
363 plants in the elevated CO_2 treatment that received 70 ppm N, one plant in the elevated CO_2
364 treatment that received 210 ppm N, two plants in the elevated CO_2 treatment that received 280
365 ppm N, two plants in the ambient CO_2 treatment that received 0 ppm N, three plants in the
366 ambient CO_2 treatment that received 70 ppm N, two plants in the ambient CO_2 treatment that
367 received 105 ppm N, and one plant in the ambient CO_2 treatment that received 280 ppm N.

A series of linear mixed-effects models were built to investigate the impacts of CO_2 concentration, nitrogen fertilization, and inoculation on *G. max* leaf nitrogen allocation, gas exchange, whole-plant growth, and investment in nitrogen fixation. All models included CO_2 treatment as a categorical fixed effect, inoculation treatment as a categorical fixed effect, and nitrogen fertilization as a continuous fixed effect, with all possible interaction terms between all three fixed effects also included. Models accounted for climatic differences between chambers across experiment iterations by including a random intercept term that nested the starting chamber rack by CO_2 treatment. Models with this independent variable structure were created for each of the following dependent variables: N_{area}, M_{area}, N_{mass}, Chl_{area}, $A_{\mathrm{net,420}}$, $A_{\mathrm{net,growth}}$, V_{cmax25}, J_{max25}, J_{max25}:V_{cmax25}, R_{d25}, $PNUE_{growth}$, χ, total leaf area, total biomass, N_{cost}, C_{bg}, N_{wp}, $\%N_{\mathrm{dfa}}$, rood nodule biomass: root biomass, root nodule biomass, and root biomass.

Shapiro-Wilk tests of normality were used to assess whether linear mixed-effects models satisfied residual normality assumptions. All models that did not satisfy residual normality assumptions satisfied such assumptions when response variables were fit using either a natural log or square root data transformation (Shapiro-Wilk: $p>0.05$ in all cases). Specifically, models for N_{area}, N_{mass}, Chl_{area}, $A_{\mathrm{net,420}}$, $A_{\mathrm{net,growth}}$, V_{cmax25}, J_{max25}, J_{max25}:V_{cmax25}, R_{d25}, $PNUE_{growth}$, χ, total leaf area, and N_{cost} each satisfied residual normality assumptions without data transformation. Models for M_{area}, total biomass, and C_{bg} satisfied residual normality assumptions with a natural log data transformation, while models for N_{wp}, root nodule biomass: root biomass, root nodule biomass, root biomass, and $\%N_{\mathrm{dfa}}$ satisfied residual normality assumptions with a square root data transformation.

In all models, we used the 'lmer' function in the 'lme4' R package (Bates *et al.*, 2015) to fit each model and the 'Anova' function in the 'car' R package (Fox & Weisberg, 2019) to calculate Type II Wald's χ^2 and determine the significance (α=0.05) of each fixed effect coefficient. We used the 'emmeans' R package (Lenth, 2019) to conduct post-hoc comparisons using Tukey's tests, where degrees of freedom were approximated using the Kenward-Roger approach (Kenward & Roger, 1997). Trendlines and error ribbons representing the 95% confidence intervals were drawn in all figures using 'emmeans' outputs across the range in nitrogen fertilization values. All analyses and plots were conducted in R version 4.1.0 (R Core Team, 2021). Model results for χ, C_{bg}, N_{wp}, root nodule biomass: root biomass, root nodule

biomass, and root biomass are reported in the *Supplemental Material* (Tables S3-S6; Figs. S3-S6).

Results

Leaf nitrogen content

Elevated CO_2 reduced N_{area}, N_{mass}, and Chl_{area} by 29%, 50%, and 31%, respectively, and increased M_{area} by 44% ($p<0.001$ in all cases; Table 1). Interactions between nitrogen fertilization and CO_2 ($p<0.05$ in all cases; Table 1) indicated that positive effects of increasing nitrogen fertilization on N_{area}, N_{mass}, and M_{area} ($p<0.001$ in all cases; Table 1) were stronger under ambient CO_2 than elevated CO_2 (Tukey test of the nitrogen fertilization-trait slope between CO_2: $p<0.05$ in all cases). These responses resulted in a stronger reduction in N_{area} and N_{mass} and a stronger increase in M_{area} under elevated CO_2 with increasing nitrogen fertilization than ambient CO_2 (Fig. S1). Nitrogen fertilization did not modify reductions in Chl_{area} due to elevated CO_2 (Tukey test of the nitrogen fertilization-Chl_{area} slope between CO_2 treatments: $p>0.05$).

An interaction between inoculation and CO_2 ($p<0.05$; Table 1) indicated that reductions in N_{area} due to elevated CO_2 were stronger in uninoculated plants (36% reduction; Tukey test of the CO_2 effect in uninoculated plants: $p<0.001$) than inoculated plants (22% reduction; Tukey test of the CO_2 effect in inoculated plants: $p<0.001$). Inoculation did not modify N_{mass}, M_{area}, or Chl_{area} responses to elevated CO_2 (CO_2-by-inoculation interaction: $p>0.05$ in all cases; Table 1). However, an interaction between nitrogen fertilization and inoculation ($p<0.05$ in all cases; Table 1; Figs. 1a-d) indicated that positive effects of increasing nitrogen fertilization on N_{area}, N_{mass}, M_{area}, and Chl_{area} ($p<0.001$ in all cases; Table 1) were stronger in uninoculated plants compared to inoculated plants (Tukey test of the nitrogen fertilization-trait slope between inoculation treatments: $p<0.05$ in all cases).

423 **Table 1** Effects of CO_2 concentration, inoculation, and nitrogen fertilization on leaf nitrogen allocation*

		N_{area}		N_{mass}		M_{area}[a]		Chl_{area}	
	df	χ^2	p	χ^2	p	χ^2	p	χ^2	p
CO_2	1	155.908	**<0.001**	272.362	**<0.001**	151.319	**<0.001**	69.233	**<0.001**
Inoculation (I)	1	86.029	**<0.001**	15.576	**<0.001**	19.158	**<0.001**	136.341	**<0.001**
N fertilization (N)	1	316.408	**<0.001**	106.659	**<0.001**	21.440	**<0.001**	163.111	**<0.001**
CO_2*I	1	4.729	**0.030**	2.025	0.155	0.029	0.866	2.102	0.147
CO_2*N	1	5.723	**0.017**	22.542	**<0.001**	7.619	**0.006**	2.999	0.083
I*N	1	43.381	**<0.001**	11.137	**0.001**	5.022	**0.025**	75.769	**<0.001**
CO_2*I*N	1	0.489	0.484	0.041	0.839	0.208	0.649	2.144	0.143

424 *Significance determined using Type II Wald χ^2 tests (α=0.05). *P*-values less than 0.05 are in bold. A superscript "[a]" is included after
425 trait labels to indicate if models were fit with natural log-transformed response variables. Key: df=degrees of freedom, χ^2=Wald chi-
426 square test statistic, N_{area}=leaf nitrogen content per unit leaf area (gN m^{-2}), N_{mass}=leaf nitrogen content (gN g^{-1}), M_{area}=leaf mass per
427 unit leaf area (g m^{-2}).
428

429 **Figure 1**

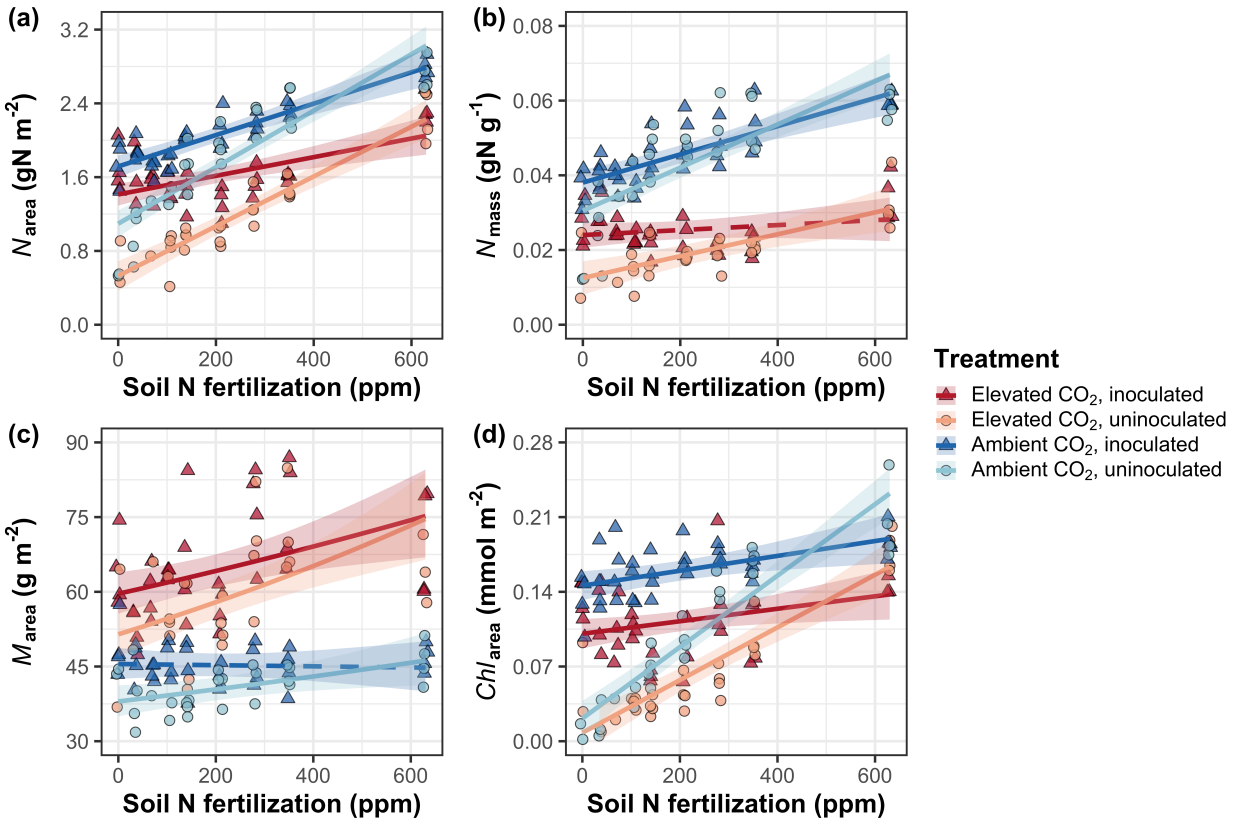

430

431 **Figure 1** Effects of CO_2 concentration, nitrogen fertilization, and inoculation on leaf nitrogen per
432 unit leaf area (a), leaf nitrogen per unit leaf mass (b), leaf mass per unit leaf area (c), and
433 chlorophyll content per unit leaf area (d). Nitrogen fertilization is represented on the x-axis in all
434 panels. Red shaded points and trendlines indicate plants grown under elevated CO_2, while blue
435 shaded points and trendlines indicate plants grown under ambient CO_2. Light blue and red
436 circular points and trendlines indicate measurements collected from uninoculated plants, while
437 dark blue and red triangular points indicate measurements collected from inoculated plants. Solid
438 trendlines indicate regression slopes that are different from zero (p<0.05), while dashed
439 trendlines indicate slopes that are not distinguishable from zero (p>0.05).

440

441 *Gas exchange*

442 Elevated CO_2 decreased $A_{net,420}$ by 17% (p<0.001; Table 2) and increased $A_{net,growth}$ by 33%
443 (p<0.001; Table 2). Nitrogen fertilization did not modify effects of elevated CO_2 on $A_{net,420}$ or
444 $A_{net,growth}$ (CO_2-by-nitrogen fertilization interaction: p>0.05 in both cases; Table 2; Fig. 2a-b).
445 Inoculation did not modify $A_{net,420}$ responses to elevated CO_2 (CO_2-by-inoculation interaction:
446 p>0.05). However, an interaction between CO_2 and inoculation (p<0.05; Table 2) indicated that
447 inoculated plants experienced a stronger increase in $A_{net,growth}$ due to elevated CO_2 (38% increase;
448 Tukey test of the CO_2 effect in inoculated plants: p<0.001) compared to uninoculated plants
449 (26% increase; Tukey test of the CO_2 effect in uninoculated plants: p<0.05). An interaction
450 between nitrogen fertilization and inoculation (p<0.001 in both cases; Table 2) indicated that
451 positive effects of increasing nitrogen fertilization on $A_{net,420}$ and $A_{net,growth}$ (p<0.001 in both
452 cases; Table 2; Fig. 2a-b) were stronger in uninoculated plants than inoculated plants (Tukey test
453 comparing the nitrogen fertilization-trait slope between inoculation treatments: p<0.001 in both
454 cases).

455 Elevated CO_2 decreased V_{cmax25} and J_{max25} by 16% and 10%, respectively, increasing
456 J_{max25}:V_{cmax25} by 8% (p<0.05 in all cases; Table 2; Fig. 2c-e). V_{cmax25}, J_{max25}, and J_{max25}:V_{cmax25}
457 responses to elevated CO_2 were not modified by nitrogen fertilization (CO_2-by-nitrogen
458 fertilization interaction: p>0.05 in all cases; Table 2; Fig. 2c-e) or inoculation (CO_2-by-
459 inoculation interaction: p>0.05 in all cases; Table 2). An interaction between nitrogen
460 fertilization and inoculation (p<0.05 in both cases; Table 2) indicated that positive effects of
461 increasing nitrogen fertilization on V_{cmax25} and J_{max25} (p<0.001 in both cases; Table 2) and
462 negative effects of increasing nitrogen fertilization on J_{max25}:V_{cmax25} (p<0.001; Table 2) were
463 driven by uninoculated plants (Tukey test of the nitrogen fertilization-trait slope in uninoculated
464 plants: p<0.001 in all cases), as there was no effect of nitrogen fertilization on V_{cmax25}, J_{max25}, or
465 J_{max25}:V_{cmax25} in inoculated plants (Tukey test of the nitrogen fertilization-trait slope in inoculated
466 plants: p>0.05 in all cases).

467 There was no effect of CO_2 concentration on R_{d25} (p>0.05; Table 2). An interaction
468 between nitrogen fertilization and inoculation (p<0.001; Table 2) indicated that the positive
469 effect of increasing nitrogen fertilization on R_{d25} (p<0.05; Table 2) was driven by uninoculated
470 plants (Tukey test of the nitrogen fertilization-R_{d25} slope in uninoculated plants: p<0.001), as

471 there was no effect of nitrogen fertilization on R_{d25} in inoculated plants (Tukey test of the
472 nitrogen fertilization-R_{d25} slope in inoculated plants: $p>0.05$).
473
474 *Photosynthetic nitrogen-use efficiency*
475 Elevated CO_2 increased $PNUE_{growth}$ by 90% ($p<0.001$; Table 2; Fig. 3), a pattern that was not
476 modified by inoculation treatment (CO_2-by-inoculation interaction: $p>0.05$; Table 2). An
477 interaction between CO_2 and nitrogen fertilization ($p<0.05$; Table 2) indicated that the positive
478 effect of elevated CO_2 on $PNUE_{growth}$ decreased with increasing nitrogen fertilization (Fig. S2).
479 This pattern was driven by a negative effect of increasing nitrogen fertilization on $PNUE_{growth}$
480 ($p<0.001$; Table 2) that was stronger under elevated CO_2 than ambient CO_2 (Tukey test
481 comparing the nitrogen fertilization-$PNUE_{growth}$ slope between CO_2 treatments: $p<0.05$). An
482 interaction between nitrogen fertilization and inoculation ($p<0.001$; Table 2; Fig. 3) indicated
483 that the negative effect of increasing nitrogen fertilization on $PNUE_{growth}$ was driven by
484 inoculated plants (Tukey test of the nitrogen fertilization-$PNUE_{growth}$ slope in inoculated plants:
485 $p<0.001$), as there was no effect of nitrogen fertilization on $PNUE_{growth}$ in uninoculated plants
486 (Tukey test of the nitrogen fertilization-$PNUE_{growth}$ slope in uninoculated plants: $p>0.05$).
487

488 **Table 2** Effects of CO_2 concentration, inoculation, and nitrogen fertilization on leaf gas exchange*

		$A_{net,420}$		$A_{net,growth}$		V_{cmax25}		J_{max25}	
	df	χ^2	*p*	χ^2	*p*	χ^2	*p*	χ^2	*p*
CO_2	1	15.747	**<0.001**	52.716	**<0.001**	18.039	**<0.001**	6.042	**0.014**
Inoculation (I)	1	77.137	**<0.001**	83.008	**<0.001**	98.579	**<0.001**	85.064	**<0.001**
N fertilization (N)	1	11.986	**<0.001**	14.658	**<0.001**	37.053	**<0.001**	25.356	**<0.001**
CO_2*I	1	1.032	0.310	5.634	**0.018**	0.065	0.799	0.667	0.414
CO_2*N	1	1.998	0.158	0.135	0.713	1.758	0.185	0.742	0.389
I*N	1	46.800	**<0.001**	50.774	**<0.001**	60.394	**<0.001**	57.41	**<0.001**
CO_2*I*N	1	0.002	0.964	1.332	0.248	0.748	0.387	0.377	0.539

		J_{max25}:V_{cmax25}		R_{d25}		$PNUE_{growth}$	
		χ^2	*p*	χ^2	*p*	χ^2	*p*
CO_2	1	92.010	**<0.001**	0.256	0.613	300.197	**<0.001**
Inoculation (I)	1	27.768	**<0.001**	3.094	0.079	9.897	**0.002**
N fertilization (N)	1	28.147	**<0.001**	5.965	**0.015**	29.695	**<0.001**
CO_2*I	1	2.916	0.088	2.563	0.109	0.944	0.331
CO_2*N	1	3.210	0.073	2.675	0.102	5.359	**0.021**
I*N	1	9.607	**0.002**	12.083	**0.001**	10.883	**<0.001**
CO_2*I*N	1	1.102	0.294	0.244	0.622	0.369	0.544

489 *Significance determined using Type II Wald χ^2 tests (α=0.05). *P*-values less than 0.05 are in bold. Key: df=degrees of freedom,
490 χ^2=Wald chi-square test statistic, A_{net}=net photosynthesis rate (μmol m^{-2} s^{-1}), V_{cmax25}=maximum rate of Rubisco carboxylation at 25°C
491 (μmol m^{-2} s^{-1}), J_{max25}=maximum rate of electron transport for RuBP regeneration at 25°C (μmol m^{-2} s^{-1}), J_{max25}:V_{cmax25}=ratio of J_{max25}
492 to V_{cmax25} (unitless), R_{d25}=dark respiration at 25°C (μmol m^{-2} s^{-1}), $PNUE_{growth}$=photosynthetic nitrogen-use efficiency (μmol CO_2 gN^{-1}
493 s^{-1})

Figure 2

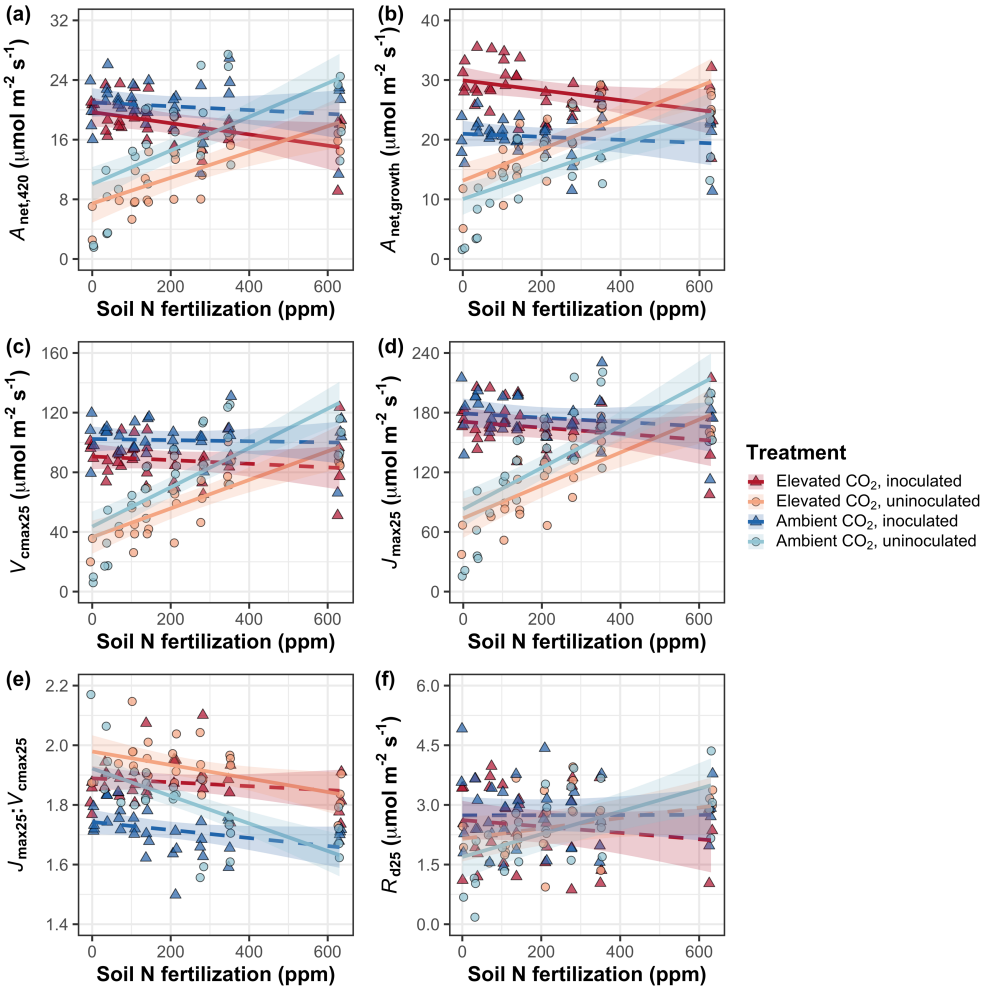

Figure 2 Effects of CO_2, nitrogen fertilization, and inoculation on net photosynthesis measured at 420 µmol mol^{-1} CO_2 (a), net photosynthesis measured under growth CO_2 concentration (b), the maximum rate of Rubisco carboxylation at 25°C (c), the maximum rate of electron transport for RuBP regeneration at 25°C (d), the ratio of the maximum rate of electron transport for RuBP regeneration to the maximum rate of Rubisco carboxylation (e), and dark respiration at 25°C (f). Nitrogen fertilization is represented on the x-axis. Red shaded points and trendlines indicate plants grown under elevated CO_2, while blue shaded points and trendlines indicate plants grown under ambient CO_2. Light blue and red circular points and trendlines indicate measurements collected from uninoculated plants, while dark blue and red triangular points indicate measurements collected from inoculated plants. Solid trendlines indicate regression slopes that are different from zero (p<0.05), while dashed trendlines indicate slopes that are not distinguishable from zero (p>0.05).

Figure 3

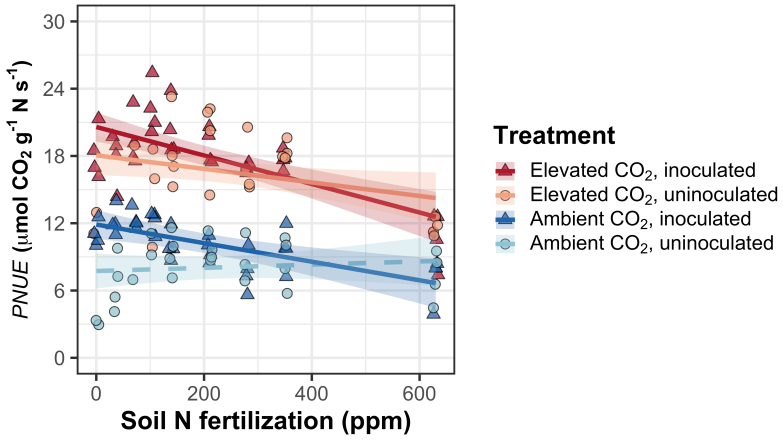

Figure 3 Effects of CO_2, nitrogen fertilization, and inoculation on photosynthetic nitrogen-use efficiency. Nitrogen fertilization is represented on the x-axis. Red shaded points and trendlines indicate plants grown under elevated CO_2, while blue shaded points and trendlines indicate plants grown under ambient CO_2. Light blue and red circular points and trendlines indicate measurements collected from uninoculated plants, while dark blue and red triangular points indicate measurements collected from inoculated plants. Solid trendlines indicate regression slopes that are different from zero ($p<0.05$), while dashed trendlines indicate slopes that are not distinguishable from zero ($p>0.05$).

519 *Whole-plant traits*

520 Elevated CO_2 increased total leaf area and total biomass by 51% and 102%, respectively
521 (p<0.001 in both cases; Table 3). Positive effects of elevated CO_2 on total leaf area and total
522 biomass were enhanced with increasing nitrogen fertilization (CO_2-by-nitrogen fertilization
523 interaction: p<0.001 in both cases; Table 3; Fig. 4a-b) but not inoculation (CO_2-by-inoculation
524 interaction: p>0.05 in both cases; Table 3). An interaction between nitrogen fertilization and
525 inoculation (p<0.001 in both cases; Table 3) indicated that positive effects of increasing nitrogen
526 fertilization on total leaf area and total biomass (p<0.001 in both cases; Table 3) were stronger in
527 uninoculated plants than inoculated plants (Tukey tests comparing the nitrogen fertilization-trait
528 slopes between inoculation treatments: p<0.05 for both traits).

529 Elevated CO_2 increased N_{cost} by 62% (p<0.001; Table 3), a pattern that was not modified
530 by nitrogen fertilization (CO_2-by-nitrogen fertilization interaction: p>0.05; Table 3). An
531 interaction between CO_2 and inoculation (p<0.05; Table 3) indicated that the positive effect of
532 elevated CO_2 on N_{cost} was stronger in uninoculated plants (99% increase; Tukey test evaluating
533 the CO_2 effect on N_{cost} in uninoculated plants: p<0.001) than inoculated plants (21% increase
534 Tukey test evaluating the CO_2 effect on N_{cost} in inoculated plants: p<0.05). An interaction
535 between nitrogen fertilization and inoculation (p<0.001; Table 3) indicated that the negative
536 effect of increasing nitrogen fertilization on N_{cost} (p<0.001; Table 3) was stronger in
537 uninoculated plants (Tukey test comparing the nitrogen fertilization-N_{cost} slope between
538 inoculation treatments: p<0.001). A three-way interaction (p<0.001; Table 3) indicated that
539 interactions between nitrogen fertilization and inoculation were stronger under elevated CO_2 than
540 ambient CO_2. This pattern was driven by greater N_{cost} in uninoculated plants grown under
541 elevated CO_2 and low nitrogen fertilization than any other CO_2-by-inoculation treatment
542 combination under low nitrogen fertilization (Tukey test comparing N_{cost} in uninoculated
543 individuals grown under elevated CO_2 and 0 ppm N to all other CO_2-inoculation treatment
544 combinations grown under 0 ppm N: p<0.001 in all cases; Fig. 4c). N_{cost} was generally reduced
545 in inoculated plants (p<0.001; Table 3). Negative effects of increasing nitrogen fertilization and
546 inoculation on N_{cost} were driven by stronger positive effects of each treatment on N_{wp} than C_{bg},
547 while positive effects of elevated CO_2 on N_{cost} were driven by stronger positive effects on C_{bg}
548 than N_{wp} (Table S4; Fig. S4).

549

550 *Nitrogen fixation*

551 Elevated CO_2 had no effect on $\%N_{dfa}$ (p=0.472; Table 3; Fig. 4d). An interaction between
552 nitrogen fertilization and inoculation (p<0.001; Table 3) indicated that the negative effect of
553 increasing nitrogen fertilization on $\%N_{dfa}$ (p<0.001; Table 3) was driven by inoculated plants
554 (Tukey test of the nitrogen fertilization-$\%N_{dfa}$ slope in inoculated plants: p<0.001), as there was
555 no effect of nitrogen fertilization on $\%N_{dfa}$ in uninoculated plants (Tukey test of the nitrogen
556 fertilization-$\%N_{dfa}$ slope in uninoculated plants: p>0.05; Fig. 4d).

557

558 **Table 3** Effects of CO_2 concentration, inoculation, and nitrogen fertilization on whole-plant growth, carbon costs to acquire nitrogen,
559 and investment toward symbiotic nitrogen fixation*

		Total leaf area		**Total biomass[b]**		**Carbon cost to acquire nitrogen**		**%N_{dfa}[b]**	
	df	χ^2	*p*	χ^2	*p*	χ^2	*p*	χ^2	*p*
CO_2	1	69.291	**<0.001**	131.477	**<0.001**	88.189	**<0.001**	0.518	0.472
Inoculation (I)	1	35.715	**<0.001**	34.264	**<0.001**	136.343	**<0.001**	955.57	**<0.001**
N fertilization (N)	1	274.199	**<0.001**	269.046	**<0.001**	80.501	**<0.001**	292.938	**<0.001**
CO_2*I	1	2.064	0.151	0.518	0.472	85.237	**<0.001**	2.010	0.156
CO_2*N	1	18.655	**<0.001**	16.877	**<0.001**	1.050	0.306	2.716	*0.099*
I*N	1	10.804	**0.001**	15.779	**<0.001**	46.489	**<0.001**	231.29	**<0.001**
CO_2*I*N	1	<0.001	0.990	0.023	0.880	18.125	**<0.001**	2.119	0.145

560 *Significance determined using Type II Wald χ^2 tests (α=0.05). *P*-values less than 0.05 are in bold and *p*-values between 0.05 and 0.10
561 are italicized. A superscript "b" after trait labels indicates if models were fit using square root transformed variables. Key: df=degrees
562 of freedom, χ^2=Wald chi-square test statistic, total leaf area (cm^2), total biomass (g), carbon cost to acquire nitrogen (gC gN^{-1}),
563 %N_{dfa}=percent leaf nitrogen content fixed from the atmosphere (%).
564

Figure 4

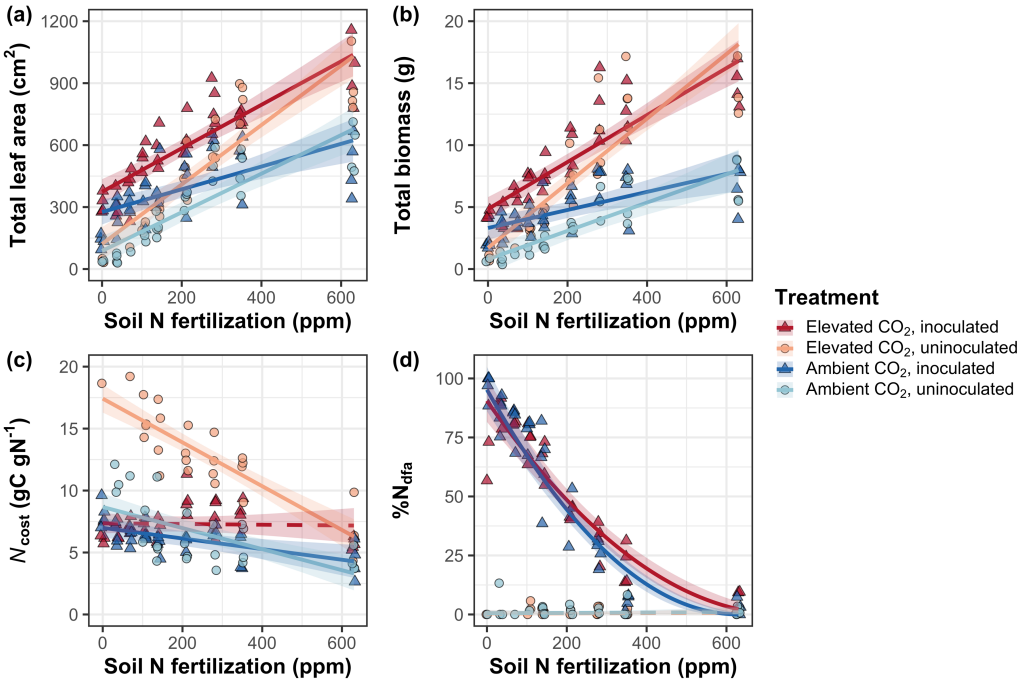

Figure 4. Effects of CO_2, nitrogen fertilization, and inoculation on total leaf area (a), total biomass (b), structural carbon costs to acquire nitrogen (c), and percent of leaf nitrogen content derived from the atmosphere (d). Nitrogen fertilization is represented on the x-axis. Red shaded points and trendlines indicate plants grown under elevated CO_2, while blue shaded points and trendlines indicate plants grown under ambient CO_2. Light blue and red circular points and trendlines indicate measurements collected from uninoculated plants, while dark blue and red triangular points indicate measurements collected from inoculated plants. Solid trendlines indicate regression slopes that are different from zero ($p<0.05$), while dashed trendlines indicate slopes that are not distinguishable from zero ($p>0.05$).

577 **Discussion**

578 *Glycine max* seedlings were grown under two CO_2 concentrations, two inoculation treatments,
579 and nine soil nitrogen fertilization treatments in a full-factorial growth chamber experiment to
580 reconcile the role of nitrogen supply, demand, and acquisition strategy on leaf and whole-plant
581 responses to elevated CO_2.

582 Results revealed that elevated CO_2 increased $A_{net,growth}$ despite reduced N_{area}, V_{cmax25}, and
583 J_{max25}. Larger reductions in V_{cmax25} than J_{max25} increased J_{max25}:V_{cmax25}, while respective increases
584 and decreases in $A_{net,growth}$ and N_{area} increased photosynthetic nitrogen-use efficiency. Effects of
585 elevated CO_2 on $A_{net,growth}$, V_{cmax25}, J_{max25}, and J_{max25}:V_{cmax25} were similar across the nitrogen
586 fertilization gradient, suggesting that leaf photosynthetic responses to elevated CO_2 were
587 decoupled from changes in nitrogen supply. Instead, increased J_{max25}:V_{cmax25} under elevated CO_2
588 indicated that plants responded to increasing atmospheric CO_2 concentrations by allowing
589 enhanced net photosynthesis rates to be achieved by approaching equal co-limitation of Rubisco
590 carboxylation rate-limited photosynthesis and electron transport for RuBP regeneration rate-
591 limited photosynthesis (Chen *et al.*, 1993; Maire *et al.*, 2012). These responses supported our
592 hypothesis that leaf photosynthetic responses to elevated CO_2 would be driven by leaf nitrogen
593 demand to build and maintain photosynthetic enzymes and would be independent of nitrogen
594 supply. Leaf photosynthetic responses to elevated CO_2 corresponded with increased total leaf
595 area and total biomass, patterns that were enhanced with increasing nitrogen fertilization and
596 associated with increased nitrogen uptake efficiency. These results supported our hypothesis that
597 whole-plant responses to elevated CO_2 would be constrained by nitrogen supply. However,
598 contrasting our hypothesis, inoculation did not modify whole-plant responses to elevated CO_2
599 due to similar plant investment in symbiotic nitrogen fixation between CO_2 treatments.

600 Combined, results indicate that nitrogen supply and demand were each important factors
601 that determined plant responses to elevated CO_2 – leaf nitrogen demand to build and maintain
602 photosynthetic enzymes drove leaf photosynthetic responses to elevated CO_2, while nitrogen
603 supply constrained whole-plant growth responses to elevated CO_2. These findings support leaf-
604 level patterns expected from eco-evolutionary optimality theory, suggesting that terrestrial
605 biosphere models may improve simulations of leaf photosynthetic processes under future novel
606 environments by considering frameworks that adopt optimality principles (Smith & Keenan,

607 2020; Harrison *et al.*, 2021; Luo *et al.*, 2021). Below, we expand and contextualize these
608 conclusions and suggest their implications for terrestrial biosphere model development.
609
610 *Nitrogen supply and demand regulate leaf and whole-plant responses to elevated CO_2 at*
611 *different scales*
612 Leaf photosynthetic responses to elevated CO_2 were consistent with previous studies that have
613 investigated or reviewed leaf responses to elevated CO_2 (Drake *et al.*, 1997; Makino *et al.*, 1997;
614 Ainsworth *et al.*, 2002; Ainsworth & Long, 2005; Ainsworth & Rogers, 2007; Crous *et al.*, 2010;
615 Lee *et al.*, 2011; Smith & Dukes, 2013; Poorter *et al.*, 2022), and follow patterns expected from
616 eco-evolutionary optimality theory (Chen *et al.*, 1993; Wright *et al.*, 2003; Maire *et al.*, 2012;
617 Prentice *et al.*, 2014; Wang *et al.*, 2017; Smith *et al.*, 2019; Smith & Keenan, 2020; Harrison *et*
618 *al.*, 2021). Positive effects of elevated CO_2 on $A_{net,growth}$ and J_{max25}:V_{cmax25} and negative effects of
619 elevated CO_2 on V_{cmax25} and J_{max25} were similar across the nitrogen fertilization gradient,
620 indicating that leaf photosynthetic responses to elevated CO_2 were decoupled from changes in
621 nitrogen supply. Increased J_{max25}:V_{cmax25} and photosynthetic nitrogen-use efficiency under
622 elevated CO_2 provide strong support for the idea that leaves were downregulating V_{cmax25} in
623 response to elevated CO_2 such that enhanced net photosynthesis rates approached becoming
624 equally co-limited by Rubisco carboxylation and RuBP regeneration (Chen *et al.*, 1993; Maire *et*
625 *al.*, 2012; Smith & Keenan, 2020). These patterns suggest that leaf photosynthetic responses to
626 elevated CO_2 were likely the result of reduced demand to build and maintain photosynthetic
627 enzymes, following patterns expected from eco-evolutionary optimality theory (Harrison *et al.*,
628 2021; Dong *et al.*, 2022b).
629 Whole-plant responses were also consistent with previous studies that have investigated
630 or reviewed whole-plant responses to elevated CO_2 (Makino *et al.*, 1997; Ainsworth *et al.*, 2002;
631 Hungate *et al.*, 2003; Ainsworth & Long, 2005; Norby *et al.*, 2010; Smith & Dukes, 2013;
632 Poorter *et al.*, 2022). Greater whole-plant growth under elevated CO_2 was associated with greater
633 carbon costs to acquire nitrogen through stronger increases in belowground carbon allocation
634 than whole-plant nitrogen uptake. These patterns indicate that plants grown under elevated CO_2
635 supported greater total leaf area and total biomass through increased plant nitrogen uptake,
636 though at reduced nitrogen uptake efficiency. Unlike leaf photosynthetic responses to elevated
637 CO_2, positive whole-plant responses to elevated CO_2 were enhanced with increasing nitrogen

638 fertilization, supporting our hypothesis that nitrogen supply would constrain whole-plant
639 responses to elevated CO_2 (Hungate *et al.*, 2003; Luo *et al.*, 2004; Finzi *et al.*, 2007). Positive
640 effects of increasing nitrogen fertilization on total leaf area and total biomass were associated
641 with reductions in carbon costs to acquire nitrogen, a pattern that was driven by stronger
642 increases in whole-plant nitrogen uptake than belowground carbon allocation (Perkowski *et al.*,
643 2021). While reductions in carbon costs to acquire nitrogen due to increasing nitrogen
644 fertilization were similar between CO_2 treatments, increasing nitrogen fertilization increased
645 whole-plant nitrogen uptake more strongly under elevated CO_2. This pattern, coupled with
646 similar effects of nitrogen fertilization on belowground carbon allocation responses to elevated
647 CO_2, indicated that stronger growth responses to elevated CO_2 with increasing nitrogen
648 fertilization were likely driven by enhanced nitrogen uptake efficiency. These findings suggest
649 that positive short-term effects of nitrogen supply on whole-plant responses to elevated CO_2 are
650 linked to reduced costs of acquiring nitrogen and increased nitrogen uptake efficiency,
651 supporting conclusions from Terrer *et al.* (2018).
652 Our findings indicate that nitrogen supply and demand could each explain plant responses
653 to elevated CO_2, though these factors operated at different scales. Specifically, photosynthetic
654 responses to elevated CO_2 were determined through reduced leaf nitrogen demand to build and
655 maintain photosynthetic enzymes. Reduced leaf nitrogen demand resulted in a shift in nitrogen
656 allocation to photosynthetic enzymes independent of soil nitrogen supply that increased
657 photosynthetic nitrogen use efficiency and allowed net photosynthesis rates to occur by
658 approaching optimal coordination of Rubisco carboxylation-limited and RuBP regeneration-
659 limited photosynthesis. Whole-plant responses to elevated CO_2 were enhanced with increasing
660 soil nitrogen supply. Interestingly, optimized nitrogen allocation to photosynthetic capacity may
661 have resulted in nitrogen savings at the leaf level that could have maximized nitrogen allocation
662 to growth. These results suggest that plants grown under elevated CO_2 responded to increased
663 nitrogen supply by increasing the number of optimally coordinated leaves and that the
664 downregulation in photosynthetic capacity under elevated CO_2 was not a direct response to
665 changes in nitrogen supply.
666
667 *Inoculation with symbiotic nitrogen-fixing bacteria does not modify leaf or whole-plant*
668 *responses to elevated CO_2*

669 Inoculation increased N_{area}, $A_{net,420}$, $A_{net,growth}$, V_{cmax25}, J_{max25}, photosynthetic nitrogen-use
670 efficiency, total leaf area, and total biomass, and decreased J_{max25}:V_{cmax25} and R_{d25}. These patterns
671 support previous literature suggesting that species that form associations with symbiotic
672 nitrogen-fixing bacteria often have increased leaf nitrogen content, photosynthetic capacity, and
673 growth compared to species that do not form such associations (Adams *et al.*, 2016; Bytnerowicz
674 *et al.*, 2023). Positive effects of inoculation on leaf and whole-plant traits were strongest under
675 low nitrogen fertilization and rapidly diminished with increasing nitrogen fertilization as
676 investment in symbiotic nitrogen fixation decreased (Andrews *et al.*, 2011; Friel & Friesen,
677 2019; McCulloch & Porder, 2021; Perkowski *et al.*, 2021), supporting the idea that nitrogen
678 fixation is a nutrient acquisition strategy that may confer competitive benefits for nitrogen-fixing
679 species growing in low soil nitrogen environments (Rastetter *et al.*, 2001; Vitousek *et al.*, 2002).
680 Interestingly, inoculation did not modify effects of elevated CO_2 on V_{cmax25}, J_{max25},
681 J_{max25}:V_{cmax25}, photosynthetic nitrogen-use efficiency, total leaf area, or total biomass. These
682 patterns corresponded with null effects of elevated CO_2 on %N_{dfa} and the ratio of root nodule
683 biomass to root biomass, suggesting that null inoculation effects on plant responses to elevated
684 CO_2 were primarily due to similar plant investments toward symbiotic nitrogen fixation between
685 CO_2 treatments. We observed these patterns regardless of nitrogen fertilization level, contrasting
686 our hypothesis that inoculation would enhance whole-plant responses to elevated CO_2 under low
687 nitrogen fertilization where individuals were expected to be invested more strongly in symbiotic
688 nitrogen fixation. These patterns also contrast previous work showing that inoculated *G. max* is
689 generally more responsive to increasing atmospheric CO_2 concentrations (Ainsworth *et al.*,
690 2002) and that plant investment toward symbiotic nitrogen fixation tends to be greater under
691 scenarios that increase whole-plant demand to acquire nitrogen (Taylor & Menge, 2018; Friel &
692 Friesen, 2019; McCulloch & Porder, 2021).
693
694 *Implications for future model development*
695 Many terrestrial biosphere models predict photosynthetic capacity through parameterized
696 relationships between N_{area} and V_{cmax} (Rogers, 2014; Rogers *et al.*, 2017), which assumes that
697 leaf nitrogen-photosynthesis relationships are constant across growing environments. Our results
698 build on previous work suggesting that leaf nitrogen-photosynthesis relationships dynamically
699 change across growing environments (Smith & Keenan, 2020; Luo *et al.*, 2021; Dong *et al.*,

2022b; Waring *et al.*, 2023), as elevated CO_2 reduced leaf nitrogen content more strongly than it increased $A_{net,growth}$ and decreased V_{cmax25} and J_{max25}. Additionally, positive effects of increasing nitrogen fertilization on indices of photosynthetic capacity were only apparent in uninoculated plants, as there was no effect of nitrogen fertilization on V_{cmax25} or J_{max25} in inoculated plants. Positive effects of increasing nitrogen fertilization on N_{area} and Chl_{area} were also markedly weaker in inoculated plants compared to uninoculated plants. These patterns indicate that leaf nitrogen-photosynthesis relationships are context-dependent on nitrogen acquisition strategy, may only be constant in environments where nitrogen supply limits leaf physiology, and will likely shift in response to increasing atmospheric CO_2 concentrations. Terrestrial biosphere models that predict photosynthetic capacity through parameterized relationships between N_{area} and V_{cmax} (e.g., Kattge *et al.*, 2009; Walker *et al.*, 2014) may risk overestimating photosynthetic capacity, therefore net primary productivity and the magnitude of the land carbon sink, under future novel growth environments.

Our results demonstrate that optimal resource allocation to photosynthetic capacity defines leaf photosynthetic responses to elevated CO_2 and that these responses are independent of nitrogen supply. Current approaches for simulating photosynthetic responses to CO_2 in terrestrial biosphere models with coupled carbon and nitrogen cycles often invoke patterns expected from progressive nitrogen limitation, where photosynthetic responses to elevated CO_2 are modeled as a function of positive relationships between nitrogen availability and leaf nitrogen content. Our results contradict this framework, suggesting that photosynthetic responses to elevated CO_2 are driven by optimal nitrogen investment to satisfy leaf nitrogen demand to build and maintain photosynthetic enzymes. Optimality models that use principles from optimal coordination and photosynthetic least-cost theories (Wang *et al.*, 2017; Stocker *et al.*, 2020; Scott & Smith, 2022) are capable of capturing responses to CO_2 independent of nitrogen supply (Smith & Keenan, 2020; Harrison *et al.*, 2021), suggesting that including optimality frameworks in terrestrial biosphere models may improve the accuracy by which photosynthetic processes are simulated in response to increasing atmospheric CO_2 concentrations.

Previous work has highlighted the fact that pot experiments restrict belowground rooting volume and may alter plant allocation responses to environmental change (Ainsworth *et al.*, 2002; Poorter *et al.*, 2012). In this study, the ratio of pot volume to total biomass was greater under elevated CO_2 and increased with increasing nitrogen fertilization such that several

731 treatment combinations exceeded values recommended by Poorter *et al*. (2012) to avoid growth
732 limitation imposed by restricted pot volume (<1 g L^{-1}; Table S6; Fig. S6). While pot size may
733 have limited plant responses to elevated CO_2, similar responses to elevated CO_2 have been
734 observed using field measurements that do not restrict belowground rooting volume (Bernacchi
735 *et al.*, 2005; Crous *et al.*, 2010; Lee *et al.*, 2011; Pastore *et al.*, 2019; Smith & Keenan, 2020).
736 Additionally, there was no apparent saturating effect of increasing fertilization on total biomass,
737 belowground carbon biomass, or root biomass under conditions where biomass: pot volume
738 ratios exceeded 1 g L^{-1} (e.g., individuals of either inoculation status grown under high
739 fertilization and elevated CO_2), which might be expected if pot volume had limited plant growth.
740 The lack of such responses indicate that the pot volume used in this study (6 L) was sufficient to
741 avoid growth limitation.
742
743 *Conclusions*
744 Our results indicate that nitrogen supply and demand each helped explain *G. max* responses to
745 elevated CO_2, though operated at different scales. Supporting eco-evolutionary optimality theory,
746 leaf photosynthetic responses to elevated CO_2 were independent of soil nitrogen supply and
747 ability to associate with symbiotic nitrogen-fixing bacteria and were instead driven by leaf
748 nitrogen demand to build and maintain photosynthetic enzymes such that net photosynthesis
749 rates approached optimal coordination. Supporting the progressive nitrogen limitation
750 hypothesis, whole-plant responses to elevated CO_2 were enhanced with increasing nitrogen
751 fertilization due to increased plant nitrogen uptake efficiency coupled with possible cascading
752 effects of nitrogen savings at the leaf level that may have maximized nitrogen allocation to
753 whole-plant growth. However, inoculation did not modify whole-plant responses to elevated
754 CO_2, as plants invested similarly in symbiotic nitrogen fixation between CO_2 treatments. Results
755 suggest that plants grown under elevated CO_2 responded to increased nitrogen supply by
756 increasing the number of optimally coordinated leaves and that the downregulation in
757 photosynthetic capacity under elevated CO_2 was not modified by changes in nitrogen supply.
758 The differential role of nitrogen supply on leaf and whole-plant responses to elevated CO_2
759 coupled with dynamic leaf nitrogen-photosynthesis relationships across CO_2 and nitrogen
760 fertilization treatments suggests that terrestrial biosphere models may improve simulations of

761 photosynthetic responses to increasing atmospheric CO_2 concentrations by adopting frameworks
762 that include optimality principles.
763
764 **Conflicts of Interest**
765 The authors declare no conflicts of interest.
766
767 **Acknowledgements**
768 This study is a contribution to the LEMONTREE (Land Ecosystem Models based On New
769 Theory, obseRvations and ExperimEnts) project, funded through the generosity of Eric and
770 Wendy Schmidt by recommendation of the Schmidt Futures programme. EAP acknowledges
771 support from a Texas Tech University Doctoral Dissertation Completion Fellowship and a
772 Botanical Society of America Graduate Student Research Award. This work was also supported
773 by US National Science Foundation awards to NGS (DEB-2045968 and DEB-2217353).
774
775 **Data Availability**
776 All R scripts, data, and metadata are available at https://doi.org/10.5281/zenodo.10177575 (or on
777 GitHub at: https://github.com/eaperkowski/NxCO2xI_ms_data)
778
779 **Author contributions**
780 EAP conceptualized the study objectives and designed the experiment in collaboration with
781 NGS, collected data, conducted data analysis, and wrote the first manuscript draft. EE assisted
782 with data collection and experiment maintenance. NGS conceptualized study objectives and
783 experimental design with EAP and oversaw experiment progress. All authors provided
784 manuscript feedback and approved the manuscript in its current form for submission to *Global*
785 *Change Biology*.
786
787 **References**
788 **Adams MA, Turnbull TL, Sprent JI, Buchmann N. 2016**. Legumes are different: Leaf
789 nitrogen, photosynthesis, and water use efficiency. *Proceedings of the National Academy of*
790 *Sciences of the United States of America* **113**: 4098–4103.
791 **Ainsworth EA, Davey PA, Bernacchi CJ, Dermody OC, Heaton EA, Moore DJ, Morgan**

PB, Naidu SL, Ra HSY, Zhu XG, *et al.* 2002. A meta-analysis of elevated [CO_2] effects on soybean (*Glycine max*) physiology, growth and yield. *Global Change Biology* **8**: 695–709.

Ainsworth EA, Long SP. **2005**. What have we learned from 15 years of free-air CO_2 enrichment (FACE)? A meta-analytic review of the responses of photosynthesis, canopy properties and plant production to rising CO_2. *New Phytologist* **165**: 351–372.

Ainsworth EA, Rogers A. **2007**. The response of photosynthesis and stomatal conductance to rising [CO_2]: mechanisms and environmental interactions. *Plant, Cell & Environment* **30**: 258–270.

Allen K, Fisher JB, Phillips RP, Powers JS, Brzostek ER. **2020**. Modeling the carbon cost of plant nitrogen and phosphorus uptake across temperate and tropical forests. *Frontiers in Forests and Global Change* **3**: 1–12.

Andrews M, James EK, Sprent JI, Boddey RM, Gross E, dos Reis FB. **2011**. Nitrogen fixation in legumes and actinorhizal plants in natural ecosystems: Values obtained using ^{15}N natural abundance. *Plant Ecology and Diversity* **4**: 117–130.

Arora VK, Katavouta A, Williams RG, Jones CD, Brovkin V, Friedlingstein P, Schwinger J, Bopp L, Boucher O, Cadule P, *et al.* 2020. Carbon-concentration and carbon-climate feedbacks in CMIP6 models and their comparison to CMIP5 models. *Biogeosciences* **17**: 4173–4222.

Barnes JD, Balaguer L, Manrique E, Elvira S, Davison AW. **1992**. A reappraisal of the use of DMSO for the extraction and determination of chlorophylls a and b in lichens and higher plants. *Environmental and Experimental Botany* **32**: 85–100.

Bates D, Mächler M, Bolker B, Walker S. **2015**. Fitting linear mixed-effects models using lme4. *Journal of Statistical Software* **67**: 1–48.

Bernacchi CJ, Morgan PB, Ort DR, Long SP. **2005**. The growth of soybean under free air [CO_2] enrichment (FACE) stimulates photosynthesis while decreasing in vivo Rubisco capacity. *Planta* **220**: 434–446.

Bernacchi CJ, Singsaas EL, Pimentel C, Portis AR, Long SP. **2001**. Improved temperature response functions for models of Rubisco-limited photosynthesis. *Plant, Cell and Environment* **24**: 253–259.

Braghiere RK, Fisher JB, Allen K, Brzostek ER, Shi M, Yang X, Ricciuto DM, Fisher RA, Zhu Q, Phillips RP. **2022**. Modeling global carbon costs of plant nitrogen and phosphorus

acquisition. *Journal of Advances in Modeling Earth Systems* **14**: 1–23.

Brzostek ER, Fisher JB, Phillips RP. **2014**. Modeling the carbon cost of plant nitrogen acquisition: Mycorrhizal trade-offs and multipath resistance uptake improve predictions of retranslocation. *Journal of Geophysical Research: Biogeosciences* **119**: 1684–1697.

Bytnerowicz TA, Funk JL, Menge DNL, Perakis SS, Wolf AA. **2023**. Leaf nitrogen affects photosynthesis and water use efficiency similarly in nitrogen-fixing and non-fixing trees. *Journal of Ecology*: 1–15.

Chen J-L, Reynolds JF, Harley PC, Tenhunen JD. **1993**. Coordination theory of leaf nitrogen distribution in a canopy. *Oecologia* **93**: 63–69.

Coleman JS, McConnaughay KDM, Bazzaz FA. **1993**. Elevated CO_2 and plant nitrogen-use: is reduced tissue nitrogen concentration size-dependent? *Oecologia* **93**: 195–200.

Crous KY, Reich PB, Hunter MD, Ellsworth DS. **2010**. Maintenance of leaf N controls the photosynthetic CO_2 response of grassland species exposed to 9 years of free-air CO_2 enrichment. *Global Change Biology* **16**: 2076–2088.

Cui E, Xia J, Luo Y. **2023**. Nitrogen use strategy drives interspecific differences in plant photosynthetic CO_2 acclimation. *Global Change Biology* **29**: 3667–3677.

Curtis PS. **1996**. A meta-analysis of leaf gas exchange and nitrogen in trees grown under elevated carbon dioxide. *Plant, Cell and Environment* **19**: 127–137.

Davies-Barnard T, Meyerholt J, Zaehle S, Friedlingstein P, Brovkin V, Fan Y, Fisher RA, Jones CD, Lee H, Peano D, *et al.* 2020. Nitrogen cycling in CMIP6 land surface models: progress and limitations. *Biogeosciences* **17**: 5129–5148.

Dong N, Prentice IC, Evans BJ, Caddy-Retalic S, Lowe AJ, Wright IJ. **2017**. Leaf nitrogen from first principles: field evidence for adaptive variation with climate. *Biogeosciences* **14**: 481–495.

Dong N, Prentice IC, Wright IJ, Evans BJ, Togashi HF, Caddy-Retalic S, McInerney FA, Sparrow B, Leitch E, Lowe AJ. **2020**. Components of leaf-trait variation along environmental gradients. *New Phytologist* **228**: 82–94.

Dong N, Prentice IC, Wright IJ, Wang H, Atkin OK, Bloomfield KJ, Domingues TF, Gleason SM, Maire V, Onoda Y, *et al.* 2022a. Leaf nitrogen from the perspective of optimal plant function. *Journal of Ecology* **110**: 2585–2602.

Dong N, Wright IJ, Chen JM, Luo X, Wang H, Keenan TF, Smith NG, Prentice IC. **2022b**.

854 Rising CO_2 and warming reduce global canopy demand for nitrogen. *New Phytologist* **235**:
855 1692–1700.
856 **Drake BG, Gonzàlez-Meler MA, Long SP**. **1997**. More efficient plants: a consequence of
857 rising atmospheric CO_2? *Annual Review of Plant Biology* **48**: 609–639.
858 **Duursma RA**. **2015**. Plantecophys - an R package for analysing and modelling leaf gas
859 exchange data. *PLOS ONE* **10**: e0143346.
860 **Eastman BA, Adams MB, Brzostek ER, Burnham MB, Carrara JE, Kelly C, McNeil BE,**
861 **Walter CA, Peterjohn WT**. **2021**. Altered plant carbon partitioning enhanced forest ecosystem
862 carbon storage after 25 years of nitrogen additions. *New Phytologist* **230**: 1435–1448.
863 **Evans JR**. **1989**. Photosynthesis and nitrogen relationships in leaves of C_3 plants. *Oecologia* **78**:
864 9–19.
865 **Evans JR, Clarke VC**. **2019**. The nitrogen cost of photosynthesis. *Journal of Experimental*
866 *Botany* **70**: 7–15.
867 **Evans JR, Seemann JR**. **1989**. The allocation of protein nitrogen in the photosynthetic
868 apparatus: costs, consequences, and control. *Photosynthesis* **8**: 183–205.
869 **Farquhar GD, von Caemmerer S, Berry JA**. **1980**. A biochemical model of photosynthetic
870 CO_2 assimilation in leaves of C_3 species. *Planta* **149**: 78–90.
871 **Farquhar GD, Ehleringer JR, Hubick KT**. **1989**. Carbon isotope discrimination and
872 photosynthesis. *Annual Review of Plant Physiology and Plant Molecular Biology* **40**: 503–537.
873 **Field CB, Mooney HA**. **1986**. The photosynthesis-nitrogen relationship in wild plants. In:
874 Givnish TJ, ed. On the Economy of Plant Form and Function. Cambridge: Cambridge University
875 Press, 25–55.
876 **Finzi AC, Moore DJP, DeLucia EH, Lichter J, Hofmockel KS, Jackson RB, Kim HS,**
877 **Matamala R, McCarthy HR, Oren R, *et al.* 2006**. Progressive nitrogen limitation of ecosystem
878 processes under elevated CO_2 in a warm-temperate forest. *Ecology* **87**: 15–25.
879 **Finzi AC, Norby RJ, Calfapietra C, Gallet-Budynek A, Gielen B, Holmes WE, Hoosbeek**
880 **MR, Iversen CM, Jackson RB, Kubiske ME, *et al.* 2007**. Increases in nitrogen uptake rather
881 than nitrogen-use efficiency support higher rates of temperate forest productivity under elevated
882 CO_2. *Proceedings of the National Academy of Sciences* **104**: 14014–14019.
883 **Firn J, McGree JM, Harvey E, Flores-Moreno H, Schütz M, Buckley YM, Borer ET,**
884 **Seabloom EW, La Pierre KJ, MacDougall AM, *et al.* 2019**. Leaf nutrients, not specific leaf

area, are consistent indicators of elevated nutrient inputs. *Nature Ecology & Evolution* **3**: 400–406.

Fox J, Weisberg S. **2019**. *An R companion to applied regression*. Thousand Oaks, California: Sage.

Friedlingstein P, Meinshausen M, Arora VK, Jones CD, Anav A, Liddicoat SK, Knutti R. **2014**. Uncertainties in CMIP5 climate projections due to carbon cycle feedbacks. *Journal of Climate* **27**: 511–526.

Friel CA, Friesen ML. **2019**. Legumes modulate allocation to rhizobial nitrogen fixation in response to factorial light and nitrogen manipulation. *Frontiers in Plant Science* **10**: 1316.

Gutschick VP. **1981**. Evolved strategies in nitrogen acquisition by plants. *The American Naturalist* **118**: 607–637.

Harrison SP, Cramer W, Franklin O, Prentice IC, Wang H, Brännström Å, de Boer H, Dieckmann U, Joshi J, Keenan TF, *et al.* 2021. Eco-evolutionary optimality as a means to improve vegetation and land-surface models. *New Phytologist* **231**: 2125–2141.

Hoagland DR, Arnon DI. **1950**. The water-culture method for growing plants without soil. *California Agricultural Experiment Station: 347* **347**: 1–32.

Hungate BA, Dukes JS, Shaw MR, Luo Y, Field CB. **2003**. Nitrogen and climate change. *Science* **302**: 1512–1513.

Katabuchi M. **2015**. LeafArea: An R package for rapid digital analysis of leaf area. *Ecological Research* **30**: 1073–1077.

Kattge J, Knorr W, Raddatz T, Wirth C. **2009**. Quantifying photosynthetic capacity and its relationship to leaf nitrogen content for global-scale terrestrial biosphere models. *Global Change Biology* **15**: 976–991.

Kenward MG, Roger JH. **1997**. Small sample inference for fixed effects from restricted maximum likelihood. *Biometrics* **53**: 983.

Kou-Giesbrecht S, Arora VK, Seiler C, Arneth A, Falk S, Jain AK, Joos F, Kennedy D, Knauer J, Sitch S, *et al.* 2023. Evaluating nitrogen cycling in terrestrial biosphere models: a disconnect between the carbon and nitrogen cycles. *Earth System Dynamics* **14**: 767–795.

LeBauer DS, Treseder K. **2008**. Nitrogen limitation of net primary productivity in terrestrial ecosystems is globally distributed. *Ecology* **89**: 371–379.

Lee TD, Barrott SH, Reich PB. **2011**. Photosynthetic responses of 13 grassland species across

11 years of free-air CO_2 enrichment is modest, consistent and independent of N supply. *Global Change Biology* **17**: 2893–2904.

Lenth R. **2019**. emmeans: estimated marginal means, aka least-squares means.

Liang J, Qi X, Souza L, Luo Y. **2016**. Processes regulating progressive nitrogen limitation under elevated carbon dioxide: a meta-analysis. *Biogeosciences* **13**: 2689–2699.

Liang X, Zhang T, Lu X, Ellsworth DS, BassiriRad H, You C, Wang D, He P, Deng Q, Liu H, *et al.* 2020. Global response patterns of plant photosynthesis to nitrogen addition: A meta-analysis. *Global Change Biology* **26**: 3585–3600.

Lu J, Yang J, Keitel C, Yin L, Wang P, Cheng W, Dijkstra FA. **2022**. Belowground carbon efficiency for nitrogen and phosphorus acquisition varies between *Lolium perenne* and *Trifolium repens* and depends on phosphorus fertilization. *Frontiers in Plant Science* **13**: 1–9.

Luo Y, Currie WS, Dukes JS, Finzi AC, Hartwig UA, Hungate BA, McMurtrie RE, Oren R, Parton WJ, Pataki DE, *et al.* 2004. Progressive nitrogen limitation of ecosystem responses to rising atmospheric carbon dioxide. *BioScience* **54**: 731–739.

Luo Y, Field CB, Mooney HA. **1994**. Predicting responses of photosynthesis and root fraction to elevated [CO_2]: interactions among carbon, nitrogen, and growth. *Plant, Cell & Environment* **17**: 1195–1204.

Luo X, Keenan TF, Chen JM, Croft H, Prentice IC, Smith NG, Walker AP, Wang H, Wang R, Xu C, *et al.* 2021. Global variation in the fraction of leaf nitrogen allocated to photosynthesis. *Nature Communications* **12**: 4866.

Maire V, Martre P, Kattge J, Gastal F, Esser G, Fontaine S, Soussana J-F. **2012**. The coordination of leaf photosynthesis links C and N fluxes in C_3 plant species. *PLoS ONE* **7**: e38345.

Makino A, Harada M, Sato T, Nakano H, Mae T. **1997**. Growth and N allocation in rice plants under CO_2 enrichment. *Plant Physiology* **115**: 199–203.

McCulloch LA, Porder S. **2021**. Light fuels while nitrogen suppresses symbiotic nitrogen fixation hotspots in neotropical canopy gap seedlings. *New Phytologist* **231**: 1734–1745.

Medlyn BE, Badeck FW, De Pury DGG, Barton CVM, Broadmeadow M, Ceulemans R, De Angelis P, Forstreuter M, Jach ME, Kellomäki S, *et al.* 1999. Effects of elevated [CO_2] on photosynthesis in European forest species: A meta-analysis of model parameters. *Plant, Cell and Environment* **22**: 1475–1495.

Meyerholt J, Sickel K, Zaehle S. **2020**. Ensemble projections elucidate effects of uncertainty in terrestrial nitrogen limitation on future carbon uptake. *Global Change Biology* **26**: 3978–3996.

Moore DJP, Aref S, Ho RM, Pippen JS, Hamilton JG, De Lucia EH. **2006**. Annual basal area increment and growth duration of *Pinus taeda* in response to eight years of free-air carbon dioxide enrichment. *Global Change Biology* **12**: 1367–1377.

Nie M, Lu M, Bell J, Raut S, Pendall E. **2013**. Altered root traits due to elevated CO_2: A meta-analysis. *Global Ecology and Biogeography* **22**: 1095–1105.

Norby RJ, Warren JM, Iversen CM, Medlyn BE, McMurtrie RE. **2010**. CO_2 enhancement of forest productivity constrained by limited nitrogen availability. *Proceedings of the National Academy of Sciences* **107**: 19368–19373.

Oreskes N, Shrader-Frechette K, Belitz K. **1994**. Verification, validation, and confirmation of numerical models in the Earth sciences. *Science* **263**: 641–646.

Paillassa J, Wright IJ, Prentice IC, Pepin S, Smith NG, Ethier G, Westerband AC, Lamarque LJ, Wang H, Cornwell WK, *et al.* 2020. When and where soil is important to modify the carbon and water economy of leaves. *New Phytologist* **228**: 121–135.

Pastore MA, Lee TD, Hobbie SE, Reich PB. **2019**. Strong photosynthetic acclimation and enhanced water-use efficiency in grassland functional groups persist over 21 years of CO_2 enrichment, independent of nitrogen supply. *Global Change Biology* **25**: 3031–3044.

Peng Y, Bloomfield KJ, Cernusak LA, Domingues TF, Prentice IC. **2021**. Global climate and nutrient controls of photosynthetic capacity. *Communications Biology* **4**: 462.

Peng Y, Prentice IC, Bloomfield KJ, Campioli M, Guo Z, Sun Y, Tian D, Wang X, Vicca S, Stocker BD. **2023**. Global terrestrial nitrogen uptake and nitrogen use efficiency. *Journal of Ecology*: 1–18.

Perkowski EA, Waring EF, Smith NG. **2021**. Root mass carbon costs to acquire nitrogen are determined by nitrogen and light availability in two species with different nitrogen acquisition strategies. *Journal of Experimental Botany* **72**: 5766–5776.

Poorter H, Bühler J, Van Dusschoten D, Climent J, Postma JA. **2012**. Pot size matters: A meta-analysis of the effects of rooting volume on plant growth. *Functional Plant Biology* **39**: 839–850.

Poorter H, Knopf O, Wright IJ, Temme AA, Hogewoning SW, Graf A, Cernusak LA, Pons TL. **2022**. A meta-analysis of responses of C_3 plants to atmospheric CO_2: dose–response curves

for 85 traits ranging from the molecular to the whole-plant level. *New Phytologist* **233**: 1560–1596.

Prentice IC, Dong N, Gleason SM, Maire V, Wright IJ. **2014**. Balancing the costs of carbon gain and water transport: testing a new theoretical framework for plant functional ecology. *Ecology Letters* **17**: 82–91.

Prentice IC, Liang X, Medlyn BE, Wang Y-P. **2015**. Reliable, robust and realistic: The three R's of next-generation land-surface modelling. *Atmospheric Chemistry and Physics* **15**: 5987–6005.

Querejeta JI, Prieto I, Armas C, Casanoves F, Diémé JS, Diouf M, Yossi H, Kaya B, Pugnaire FI, Rusch GM. **2022**. Higher leaf nitrogen content is linked to tighter stomatal regulation of transpiration and more efficient water use across dryland trees. *New Phytologist* **235**: 1351–1364.

R Core Team. **2021**. R: A language and environment for statistical computing.

Rastetter EB, Vitousek PM, Field CB, Shaver GR, Herbert D, Ågren GI. **2001**. Resource optimization and symbiotic nitrogen fixation. *Ecosystems* **4**: 369–388.

Reich PB, Hobbie SE, Lee T, Ellsworth DS, West JB, Tilman D, Knops JMH, Naeem S, Trost J. **2006**. Nitrogen limitation constrains sustainability of ecosystem response to CO_2. *Nature* **440**: 922–925.

Rogers A. **2014**. The use and misuse of $V_{c,max}$ in Earth System Models. *Photosynthesis Research* **119**: 15–29.

Rogers A, Medlyn BE, Dukes JS, Bonan GB, Caemmerer S, Dietze MC, Kattge J, Leakey ADB, Mercado LM, Niinemets Ü, *et al.* 2017. A roadmap for improving the representation of photosynthesis in Earth system models. *New Phytologist* **213**: 22–42.

Saathoff AJ, Welles J. **2021**. Gas exchange measurements in the unsteady state. *Plant Cell and Environment* **44**: 3509–3523.

Sage RF. **1994**. Acclimation of photosynthesis to increasing atmospheric CO_2: The gas exchange perspective. *Photosynthesis Research* **39**: 351–368.

Schneider CA, Rasband WS, Eliceiri KW. **2012**. NIH Image to ImageJ: 25 years of image analysis. *Nature Methods* **9**: 671–675.

Scott HG, Smith NG. **2022**. A Model of C4 Photosynthetic Acclimation Based on Least-Cost Optimality Theory Suitable for Earth System Model Incorporation. *Journal of Advances in*

Modeling Earth Systems **14**: 1–16.

Shi M, Fisher JB, Brzostek ER, Phillips RP. **2016**. Carbon cost of plant nitrogen acquisition: Global carbon cycle impact from an improved plant nitrogen cycle in the Community Land Model. *Global Change Biology* **22**: 1299–1314.

Smith NG, Dukes JS. **2013**. Plant respiration and photosynthesis in global-scale models: incorporating acclimation to temperature and CO_2. *Global Change Biology* **19**: 45–63.

Smith NG, Keenan TF. **2020**. Mechanisms underlying leaf photosynthetic acclimation to warming and elevated CO_2 as inferred from least-cost optimality theory. *Global Change Biology* **26**: 5202–5216.

Smith NG, Keenan TF, Prentice IC, Wang H, Wright IJ, Niinemets Ü, Crous KY, Domingues TF, Guerrieri R, Ishida FY, *et al.* 2019. Global photosynthetic capacity is optimized to the environment. *Ecology Letters* **22**: 506–517.

Smith SE, Read DJ. **2008**. *Mycorrhizal Symbiosis*.

Stocker BD, Wang H, Smith NG, Harrison SP, Keenan TF, Sandoval D, Davis T, Prentice IC. **2020**. P-model v1.0: An optimality-based light use efficiency model for simulating ecosystem gross primary production. *Geoscientific Model Development* **13**: 1545–1581.

Taylor BN, Menge DNL. **2018**. Light regulates tropical symbiotic nitrogen fixation more strongly than soil nitrogen. *Nature Plants* **4**: 655–661.

Terrer C, Vicca S, Hungate BA, Phillips RP, Prentice IC. **2016**. Mycorrhizal association as a primary control of the CO_2 fertilization effect. *Science* **353**: 72–74.

Terrer C, Vicca S, Stocker BD, Hungate BA, Phillips RP, Reich PB, Finzi AC, Prentice IC. **2018**. Ecosystem responses to elevated CO_2 governed by plant–soil interactions and the cost of nitrogen acquisition. *New Phytologist* **217**: 507–522.

Vitousek PM, Cassman K, Cleveland CC, Crews T, Field CB, Grimm NB, Howarth RW, Marino R, Martinelli L, Rastetter EB, *et al.* 2002. Towards an ecological understanding of biological nitrogen fixation. In: The Nitrogen Cycle at Regional to Global Scales. Dordrecht: Springer Netherlands, 1–45.

Vitousek PM, Howarth RW. **1991**. Nitrogen limitation on land and in the sea: How can it occur? *Biogeochemistry* **13**: 87–115.

Walker AP, Beckerman AP, Gu L, Kattge J, Cernusak LA, Domingues TF, Scales JC, Wohlfahrt G, Wullschleger SD, Woodward FI. **2014**. The relationship of leaf photosynthetic

traits - V_{cmax} and J_{max} - to leaf nitrogen, leaf phosphorus, and specific leaf area: a meta-analysis and modeling study. *Ecology and Evolution* **4**: 3218–3235.

Wang H, Prentice IC, Keenan TF, Davis TW, Wright IJ, Cornwell WK, Evans BJ, Peng C. **2017**. Towards a universal model for carbon dioxide uptake by plants. *Nature Plants* **3**: 734–741.

Waring EF, Perkowski EA, Smith NG. **2023**. Soil nitrogen fertilization reduces relative leaf nitrogen allocation to photosynthesis. *Journal of Experimental Botany* **74**: 5166–5180.

Wellburn AR. **1994**. The spectral determination of chlorophylls a and b, as well as total carotenoids, using various solvents with spectrophotometers of different resolution. *Journal of Plant Physiology* **144**: 307–313.

Westerband AC, Wright IJ, Maire V, Paillassa J, Prentice IC, Atkin OK, Bloomfield KJ, Cernusak LA, Dong N, Gleason SM, *et al.* 2023. Coordination of photosynthetic traits across soil and climate gradients. *Global Change Biology* **29**: 856–873.

Wieder WR, Cleveland CC, Smith WK, Todd-Brown K. **2015**. Future productivity and carbon storage limited by terrestrial nutrient availability. *Nature Geoscience* **8**: 441–444.

Wright IJ, Reich PB, Westoby M. **2003**. Least-cost input mixtures of water and nitrogen for photosynthesis. *The American Naturalist* **161**: 98–111.

Zaehle S, Medlyn BE, De Kauwe MG, Walker AP, Dietze MC, Hickler T, Luo Y, Wang YP, El-Masri B, Thornton P, *et al.* 2014. Evaluation of 11 terrestrial carbon-nitrogen cycle models against observations from two temperate Free-Air CO_2 Enrichment studies. *New Phytologist* **202**: 803–822.